

SUPERPLASTIC CREEP IN THE

LEAD TIN EUTECTIC

by

ALBERT KEITH SURGES

B.A. Sc., University of British Columbia, 1967

A THESIS SUBMITTED IN PARTIAL FULFILMENT OF

THE REQUIREMENTS FOR THE DEGREE OF

MASTER OF APPLIED SCIENCE

in the Department

of

METALLURGY

We accept this thesis as conforming to the

required standard

THE UNIVERSITY OF BRITISH COLUMBIA

August, 1969

In presenting this thesis in partial fulfilment of the requirements for an advanced degree at the University of British Columbia, I agree that the Library shall make it freely available for reference and study.

I further agree that permission for extensive copying of this thesis for scholarly purposes may be granted by the Head of my Department or by his representatives. It is understood that copying or publication of this thesis for financial gain shall not be allowed without my written permission.

Department of Metallurgy

The University of British Columbia
Vancouver 8, Canada

Date October 27, 1970

Abstract

An extensive creep study of a superplastic material has not previously been made. The present study was carried out to determine if there are any basic differences between the creep of coarse grained materials and fine grained superplastic materials. The results give information about the mechanical properties of superplastic alloys and are relevant to an understanding of the mechanics of superplasticity.

At high strain rates the superplastic lead-tin eutectic deforms by recovery creep and a 3-stage creep curve is observed, similar to that found for coarse grained materials. As the strain rate is decreased, the initial transient (primary creep) disappears and the creep curve is linear until necking occurs and tertiary creep ends in failure. In the principal superplastic range, at medium strain rates, creep curves are linear to at least 50 % strain. The recovery rate is immediately equal to the strain hardening rate and there is no primary creep. At low strain rates the creep curve is slightly convex as the creep rate decreases with time. This may be due to the self extinguishing nature of diffusional creep or possibly strain induced grain growth.

These results are consistent with the grain boundary sliding theories of superplasticity although details of the accommodation processes are not known. At the lowest strain rates, diffusional creep may operate.

ACKNOWLEDGMENT

The author is grateful for the advice of and helpful discussion with his research director, Dr. T.H. Alden. Thanks are also extended to R.C. Cook and K.C. Donaldson for their discussions and suggestions. C.B. Sullivan's assistance with draghting for the presentation of this thesis is also appreciated.

TABLE OF CONTENTS

1.	INTRODUCTION	1
1.1	Stage II (Superplastic Stage)	3
1.1.1	Review of Experiment	3
1.1.2	Theoretical Discussion	5
1.2	Stage III	6
1.3	Stage I	6
1.4	Previous Creep Studies on Lead and Tin Systems ...	8
2.	EXPERIMENTAL	9
2.1	Material and Specimen Preparation	9
2.2	Creep Tests	10
3.	RESULTS	13
3.1	Calculations	13
3.2	Log Stress versus Log Strain Rate Curves	13
3.3	Creep Curves	16
3.3.1	Stage II Creep Curves	16
3.3.2	Stage I Creep Curves	17
3.3.3	Stage II - Stage III Transition Creep Curves	17
3.3.4	Stage III Creep Curves	23
3.4	Incremental Loading and Unloading	23
3.5	Strain After-Effects	29
4.	DISCUSSION	30
4.1	Stage III	30
4.2	Stage III - Stage II Transition	35
4.3	Stage III	37
4.4	Stage I	40
5.	SUMMARY AND CONCLUSIONS	44
6.	SUGGESTIONS FOR FUTURE WORK	46
7.	APPENDICES	47
7.1	Computer Programme	47
7.2	Additional Creep Curves.....	52

7.3	Calculation of Theoretical Creep Curves for Pure Nabarro-Herring Creep and Pure Coble Creep	53
8.	BIBLIOGRAPHY	64

LIST OF FIGURES

<u>No.</u>	<u>Page</u>
1. Characteristic log stress versus log strain rate curve.	1
2. Specimen in grips.	10
3. Constant stress creep machine.	12
4. Log stress versus log strain rate curve. (SGS, 2 microns).	14
5. Log stress versus log strain curve. (LGS, 8 microns).	15
6. Comparison of the S-curve data of the present and previous work.	16
7. Stage II creep curve (SGS), 429 psi.	18
8. Stage II creep curve (SGS), 1716 psi.	19
9. Stage II creep curve (SGS), 715 psi.	20
10. Stage II creep curve (LGS), 814 psi.	21
11. Stage I creep curve (SGS), 97 psi.	22
12. Creep curve in stage II-stage II transition (SGS, 3432 psi.	24
13. Creep curve in stage II-stage III transition (LGS), 3582 psi.	25
14. Stage III creep curve (5212 psi).	26
15. Stage III creep curve (5535 psi).	26
16. Stage III creep curve (6512 psi).	28
17. Strain required to reach steady state versus creep stress.	27
18. Incremental loading during superplastic creep.	18
19. Return of an initial transient with incremental loading in stage III	31
20. Transition to steady state with unloading in stage III.	31
21. Strain relaxation study in stage II	32
22. Reloading after recovery in stage III	32
23. Log stress versus log strain rate relationship for Pb-2.45 wt%.	

24. Log stress versus log strain rate relationship for Pb-2.45 wt% thallium (100 μ).
25. Experimental, theoretical N-H and theoretical Coble creep curves (97 psi). 43

Appendix III

- a. Stage II (SGS) 572 psi.
- b. Stage II (SGS), 858 psi.
- c. Stage II (SGS), 1144 psi.
- d. Stage II LGS), 407 psi.
- e. Stage II (LGS), 1221 psi.
- f. Stage I (SGS), 120 psi.
- g. Stage I (SGS), 143 psi.
- h. Stage I (SGS), 286 psi.
- i. Transition (SGS), 2574 psi.
- j. Transition (SGS), 2860 Psi.
- k. Transition (LGS), 1954 psi.
- l. Transition (LGS), 2280 psi.
- m. Transition (LGS), 2606 psi.
- n. Transition (LGS), 2932 psi.
- o. Transition (LGS), 32580 psi.
- p. Transition (LGS), 3908 psi.
- q. Transition (LGS), 4234 psi.
- r. Transition (LGS), 4560 psi.
- s. Transition (LGS), 4886 psi.
- t. Stage III, 2931 psi.
- u. Stage III, 7326 psi.
- v. Stage II incremental loading.
- w. Stage III unloading

1. Introduction

Superplastic behaviour has been found in many metal systems. Alloys of lead and zinc have been investigated most frequently, but systems containing nickel, iron, aluminium, tin, cadmium, magnesium, and copper have also exhibited superplastic properties. Studies have also been made to determine deformation mechanisms which are consistent with experiment. Results of these studies may also be important in the development of new metal-forming techniques.

Stress versus strain rate results from tensile and creep tests have been plotted as log stress ($\log \sigma$) versus log strain rate ($\log \dot{\epsilon}$) to produce a characteristic three stage S-shaped curve. In the superplastic range, stage II, the strain rate ($\dot{\epsilon}$) is insensitive to the applied stress (σ).

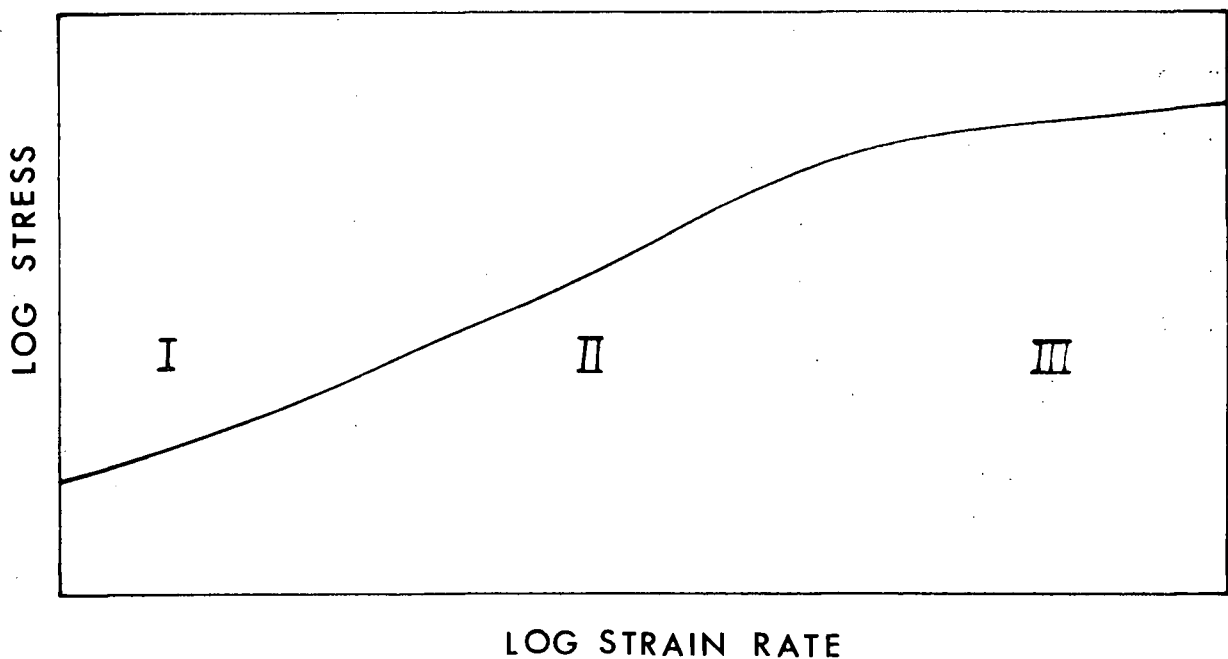


Figure 1. Characteristic log stress - log strain rate curve.

Each stage of the S-curve may be described by the equation

$$\sigma = K\dot{\epsilon}^m \quad (1)$$

where K is a constant and m is called the strain rate sensitivity parameter. Typical values of m vary from less than .1 for most metals up to 1.0 for hot polymers and glasses. Superplastic metals have been observed to exhibit m values as high as .85¹, but are typically about 0.5. In stage II, where m is high, propagation of a neck is prevented by a local hardening resulting from an increased strain rate, and thus deformation will proceed in a softer portion of the material. Accordingly, a high value of m is associated with large elongations, reportedly as high as 2000 %².

Mathematically, the relationship between m and elongation can be shown more explicitly by first differentiating equation (1) to obtain

$$\frac{d\dot{\epsilon}}{\dot{\epsilon}} = \frac{1}{m} \left[\frac{d\sigma}{\sigma} - \log\left(\frac{\sigma}{K}\right) \frac{dm}{m} \right] \quad (2)$$

It can be seen that the larger the value of m, the more insensitive strain rate becomes to a change in stress. Also, over a certain strain rate range in superplastic materials, m increases slightly with increasing strain rate. The positive variation of m in superplastic materials will cause the factor in brackets in equation (2) to be reduced, and will further reduce sensitivity to necking.

Further description of experimental and theoretical studies on superplasticity is most conveniently done by considering the stages of the $\log \sigma - \log \dot{\epsilon}$ curve separately. Of these, the most important and intensively studied is stage II.

1.1. Stage II (Superplastic Stage)

1.1.1. Review of Experiment

A fine grain size has been shown to be the most important microstructural requirement for superplasticity.³⁻¹¹ Providing the phases are of comparable hardness, the composition and means by which grain refinement is achieved are of secondary importance.^{6,9} In two phase systems, a hot or cold working step will permit the formation of a fine grain size, while phase boundaries inhibit grain growth. Thus extensive studies have been made on the eutectoid Zn - 22 wt. % Al and the Pb-Sn systems. Dilute alloy^{4-6,14-16} and pure metal^{6,17} systems have also exhibited superplasticity. The inherent problem with these systems is to produce and maintain a finely-divided microstructure. For a given time and temperature, grain size is larger in dilute alloys.

Large elongations during stage II have been consistently reported. The largest elongations occur at strain rates near that associated with peak m values^{16,18}. Maximum elongation may occur precisely at peak m but the result is obscured by the decreasing strain rate during a tensile test on a constant cross-head rate machine such as an Instron.

Tensile tests involving several grain sizes show that the effect of grain coarsening is to shift the strain rate at constant stress to lower values. This shift is expressed by the relationship $\dot{\epsilon} \sim 1/L^\alpha$ (for constant m) where α is usually between 2 and 4^{1,3,5,7,8,12,13} and L is the spacing between grain or phase boundaries.

Temperature also has an effect on the S-curve. The maximum m for each temperature drops with decreasing temperature¹. The strain rate corresponding to peak m also decreases with decreasing temperature. An increase in tempera-

ture shifts the curve to higher strain rates and to slightly lower stresses.

Grain boundary sliding is observed and its contribution to total strain increases as the strain rate is lowered from stage III into stage II^{5,11}. Experimentally, the contribution of GBS to total strain is determined by measuring the offset of grid lines inscribed across grain boundaries prior to deformation. Superplastic deformation does not cause the build up of a dislocation substructure. An Mg-Al alloy¹ has been water quenched from 400°C during superplastic deformation and transmission electron microscopy showed no dislocation traces. Dislocations are present after deformation in stage III. The low temperature yield stress remains unchanged, relative to that of the undeformed material, after stage II deformation¹³. Pb-5% Cd specimens were deformed 2 % at a selected temperature, strain rate and grain size and immediately quenched to -90°C. The .2% yield stress was then determined. Specimens deformed in the superplastic range showed no increase in yield stress while those deformed in stage III showed an increase in yield stress.

Grain shape remains equiaxed after as much as 1000 % elongation⁵. Grain growth occurs^{16,19} and may be important in the deformation process or may mask other relationships.

Recovery rates are fast in superplastic materials¹³ and decrease with increasing grain size. Pb-5% Cd specimens were deformed 2% at -90°C, annealed for various times at 50°C then deformed again at -90°C. The amount of recovery, R, was determined by $R = (\sigma_H - \sigma_R) / (\sigma_H - \sigma_Y)$, where σ_H is determined after 2% strain, σ_R after recovery and σ_Y on the annealed material. There was 40% recovery for a 4.1 μ grain size after only .2 minutes while it took 100 minutes to obtain 30 % recovery in a 15 μ specimen.

Although there is general agreement in the experimental observations made on superplastic materials, disagreement on the relative importance or interpretation of individual observation has lead to a wide range of suggested mechanisms.

1.1.2. Theoretical Discussion

Work on the Al-33 wt. % Cu eutectic⁷ and the Zn-Al eutectic¹¹ lead to similar proposals that the high strain rate sensitivity which characterizes superplasticity is the result of boundary shearing and migration. Grain boundary shear was suggested to be rate controlling, and mechanical obstructions to sliding were removed by strain rate enhanced boundary migration and recrystallization. At this intermediate strain rate, boundaries become smoother and stress is determined by viscous drag along the boundaries. Work on the Pb-Sn⁶ and Sn-Bi⁵ systems also lead to the proposal that grain boundary sliding was the rate controlling mechanism. Experimental results showed⁶ that the greatest contribution of grain boundary sliding occurred when the strain rate sensitivity parameter, m , reached its peak value. Another suggested mechanism for deformation of Pb-Sn¹⁰ incorporates non-Newtonian grain boundary sliding and diffusional (Newtonian) creep acting together in parallel and then in series with non-Newtonian slip creep. Close reproduction of an experimental $\log \sigma - \log \dot{\epsilon}$ curve, obtained by using new and previously plotted⁶ points, could be made using semi-empirical procedures based on the model.

Grain boundary sliding was proposed to explain the superplastic behaviour of the Mg-Al eutectic by Lee¹. GBS is accompanied by grain deformation and recovery. These cooperative processes are necessary, especially in regions near the boundary, to permit extensive plastic deformation. No dislocations

were seen after superplastic deformation. This is possible because the fine grain size permits all dislocations, even in the bulk of a grain, to be attracted to ^{20,21} and reach a boundary which is sliding by dislocation movement ^{22,13} or diffusional processes ²⁴, and be annihilated. It is suggested that this model might explain the low amounts of GBS during bicrystal sliding experiments ^{25,26} where the effective grain size is more or less infinite, thus limiting recovery to regions near the grain boundary.

Another model ³, based on experimental work on Pb-Sn, involves two competing processes. These are Nabarro-Herring (N-H) creep, and dislocation motion. In the high m region, the N-H model is dominant and flow is strongly viscous. A modification ²⁷ of this model, involving the Coble variant of the N-H analysis which is based on grain boundary diffusion rather than volume diffusion, was suggested to better account for the observed strain rates.

1.2. Stage III

This region at the high strain rate end of the S-curve is not superplastic. Low m values are typical. There seems to be little controversy as to the mode of deformation present. Slip is the deformation process indicated from photomicrographs and electron micrographs which show slip lines and dislocation structures remaining after deformation. The controlling process is probably recovery by dislocation climb.

1.3. Stage I

Stage I shows grain elongation ^{7,28}, striations ¹⁰ or denuded zones ²⁹ at transverse boundaries, and reduced grain boundary sliding ^{1,11}. There has been some question as to whether this stage is representative of a separate

mechanism or is at least partially a continuation of stage II. Further study over a wider range of variables may explain the true relationship. Study of deformation in this region often requires long term creep tests because of the low strain rates involved.

Chaudhari³⁰ proposes that in stage I the dislocation density is small and the dislocations reaching the grain boundary can be absorbed at the boundary by either sliding or migration and local dislocation climb. As the stress is increased, the flux of dislocations approaching a grain boundary increases more rapidly than does the ability of the grain boundary to absorb them. This results in a dislocation buildup, an internal stress which increases with strain rate and finally stage II where stress increases rapidly with strain rate.

Deformation of the Mg-Al eutectic at a low strain rate was studied by Lee¹. He found deformation to be a combined effect of grain deformation and deformation across transverse grain boundaries. The latter made up 1/3 of the deformation and occurred by GBS and possibly some diffusional creep.

Alden³¹ has recently proposed that slip at triple lines in response to sliding is rate controlling. The model involves the viscous glide of dislocations between a source (the triple line) and a perfect sink (the opposite grain boundary) and predicts an m value between .33 and .5 and an activation energy of bulk diffusion. He suggests that superplastic creep of Fe-Ni-Cr may be of this type. Fe-Ni-Cr and Zn-Al (40.6 at.% Al eutectoid) show only 2-stage $\log \sigma$ curves. Alden suggests that stage II is not energetically favorable and only stages I and III are seen in these systems.

Constant load creep tests on the 2-stage Zn-Al eutectic lead Chaudhari³² to the conclusion that a dislocation model was involved at temperatures above 200°C. The model involved the motion of dislocations in an internal stress field generated by neighbouring dislocations. Experiment showed that above 200°C the strain rate is controlled by a thermally activated process with an activation energy of 35.3 k cal./g-atom; below 175°C, by a thermally activated process with an activation energy of 21k-cal./g-atom. These values are close to those associated with bulk diffusion in Al and Zn respectively.

Zehr and Backofen¹⁰ represent stage I by a non-Newtonian dashpot model. They assign an m value .33 and plot a line on the $\log \sigma - \log \dot{\epsilon}$ curve but state that its rationale is no more than speculative.

1.4 Previous Creep Studies on Lead and Tin Systems

The present work was carried out on the eutectic Pb-Sn alloy of fine grain size. Constant stress creep testing was chosen to determine if this method would show any difference between the creep of superplastic and non-superplastic materials. All reported creep work on lead, tin and lead-tin has involved large grain size materials. In lead³³ slip occurred at the initiation of creep and a time $1/3$ law was obeyed until recrystallization³⁴ occurred. A three stage creep curve was found. Work³⁵ on the Pb-Sn eutectic, and on pure tin and lead, always showed a 3-stage creep curve. It was suggested that primary creep must always occur.

Creep studies on large grained tin³⁶ at stresses between 629 and 1394 psi and 22 and 224.5°C always resulted in 3-stage creep curves.

If a material is totally unloaded after deformation, its shape changes with time beyond an initial predominantly elastic recovery and tends to approach its initial shape. This is known as the "anelastic after effect". This effect is shown by Garofalo for lead³⁷ at 25°C where 25 % of the deformation is recovered.

Most reported stress versus strain rate data has been obtained using a tensile testing machine. This results in strain rate decreasing and stress changing with time. The results of these tests are not usually reported with a statement indicating whether corrections were made for these effects inherent in the tensile testing machine. It is also difficult to determine a "steady state" with the tensile machine. A creep test should avoid these difficulties.

2. EXPERIMENTAL

2.1. Material and Specimen Preparation

Ingots of the Pb-Sn eutectic (61.9 % Sn) were cast in graphite molds under argon. Materials of 99.99 % purity or better were used. Ingot dimensions were 5/8 inch diameter and 5 inches long.

The surface of the cast billets was machined and the material was extruded at room temperature into rods of .099 and .083 inch diameter. The first and last 18 inches of the extrusions were discarded. The rod was then cut into 3½ inch lengths. Samples of .099 inch diameter rods were roughened at each end with emery paper and epoxied into brass grips (Fig.2) with Epon 828 epoxy resin. The grips were drilled one inch deep with a .113 inch drill and the hole was tapped to improve the epoxy bond. These specimens were aged

7 days at room temperature and then stored in liquid nitrogen. The length of time of testing was generally small compared to the total time at room temperature so that grain growth during testing at room temperature was minimized. Rods of .083 inch diameter were sealed in evacuated glass tubes and were annealed at $165 \pm 2^{\circ}\text{C}$ for 30 days in an oil bath to produce grain growth. These rods were also epoxied into brass grips with a .1015 inch tapped hole. These specimens were stored at room temperature.

Comparison of log stress versus log strain rate curves previously presented for this material^{6,10} with those resulting from this study shows the small grain size material (SGS) to have a grain size of 2 microns while the large grain size material (LGS) has a grain size of 8 microns.

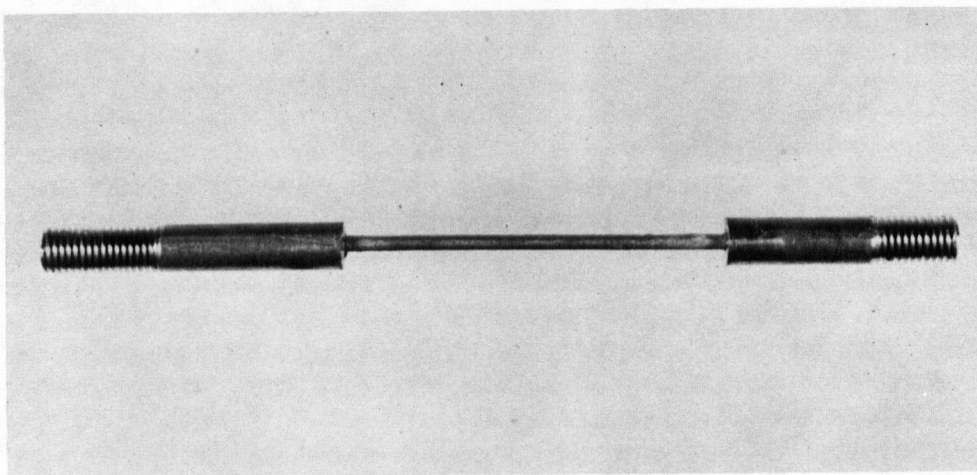


Figure 2. Specimen in grips

2.2. Creep Tests

Creep tests were performed on a constant stress machine (Figure 3). The cam design has a mechanical advantage such that the load on the specimen is twice that in the weight bucket. The constant stress cam is designed for a specimen gauge length of 25 mm. The applied load was transmitted to the

specimen by a chromel tape which followed the contour of the cam exactly rather than tending to bow as round wires were found to do. The maximum elongation possible with this creep machine corresponded to 50 percent true strain. Loading and unloading operations were carried out by lowering and raising a scissor jack under the weight bucket. All tests were done at room temperature ($22 \pm 1^{\circ}\text{C}$).

Elongation measurements were made with both a travelling optical microscope and an extensometer which was connected to a modified Heathkit recorder and attached to the sample with knife edges. Elongations could be measured to $\pm .001$ cm with the microscope and to within .0002 inches with the extensometer and recorder.

The microscope was used to follow the elongation of specimens deforming under low stresses. Measurement was made of the displacement of a single mark inscribed on the specimen grip with a razor blade. Experiment showed that there was no slippage in the grips and that it was not necessary to observe the travel of two marks on the specimen itself.

The extensometer was used at higher stresses and strain rates where automatic continuous recording was essential. No significant extensometer knife edge indentation occurred at these strain rates.

The load was increased or decreased during some tests to determine the effect of stress changes on the resulting creep curves. At high stresses, involving the large grain size material, changes in stress were made during the initial transient of the creep curves. Specimens were also suddenly unloaded and the gauge length was recorded with the extensometer to determine if unloading transients existed over any stress range.

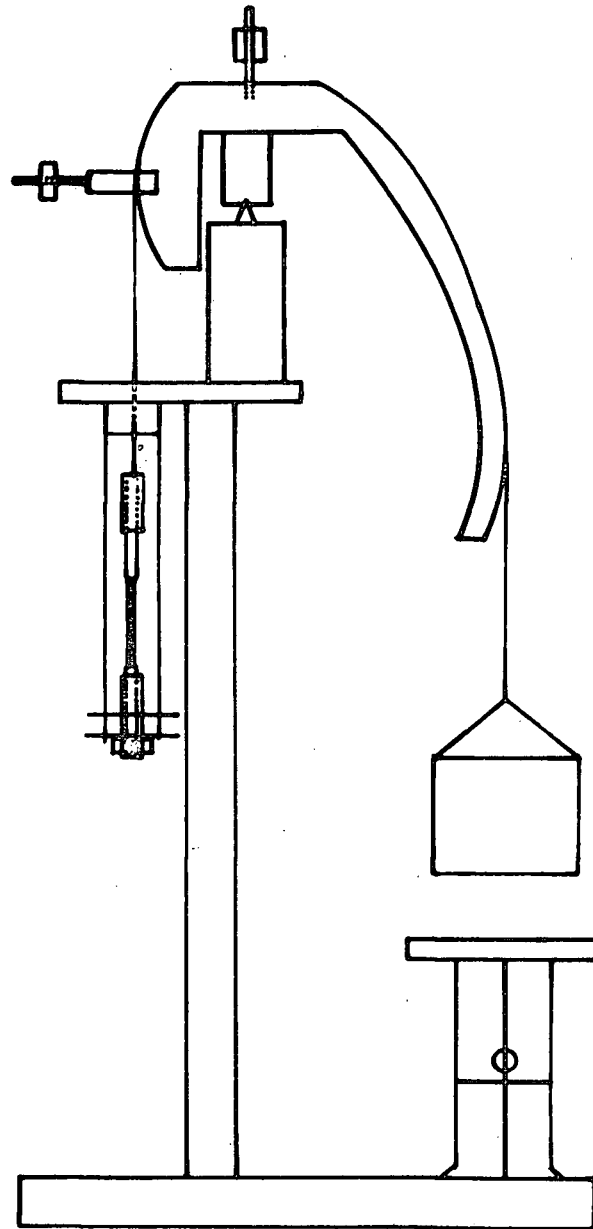


Figure 3. Constant stress creep machine.

3. RESULTS

3.1. Calculations

All calculations were done on an IBM 360 computer. The programme is shown in Appendix I. Key punched data included initial gauge length, and elongations at a series of times (hours). A scale factor was included to convert deflections on the Heathkit recorder, used with the extensometer, to inches. The computer output included a scaled creep curve plot of true strain versus time and strain rate versus time. Also included was a printed table listing each true strain, strain rate and time point plotted.

Initially, high strain rate values which fall off very quickly may be due to straightening of the specimen. This effect should be maximum when a large gauge length is used as was done with tests using the travelling microscope. Elastic strain would also contribute to this result. These effects could not be isolated and remain in the computer output.

Plots of strain rate are determined from the strain rate between two successive points. This results in a jagged strain rate curve. The strain rate scale is often expanded and this also tends to make the resulting curve jagged.

3.2. Log Stress versus Log Strain Rate Curves

Strain rate data obtained from creep tests were used to obtain log stress versus log strain rate plots for each grain size. These plots are shown in Figures 4 and 5. Strain rate values used were the initial strain rate in stages I and II and the steady state creep rate in stage III.

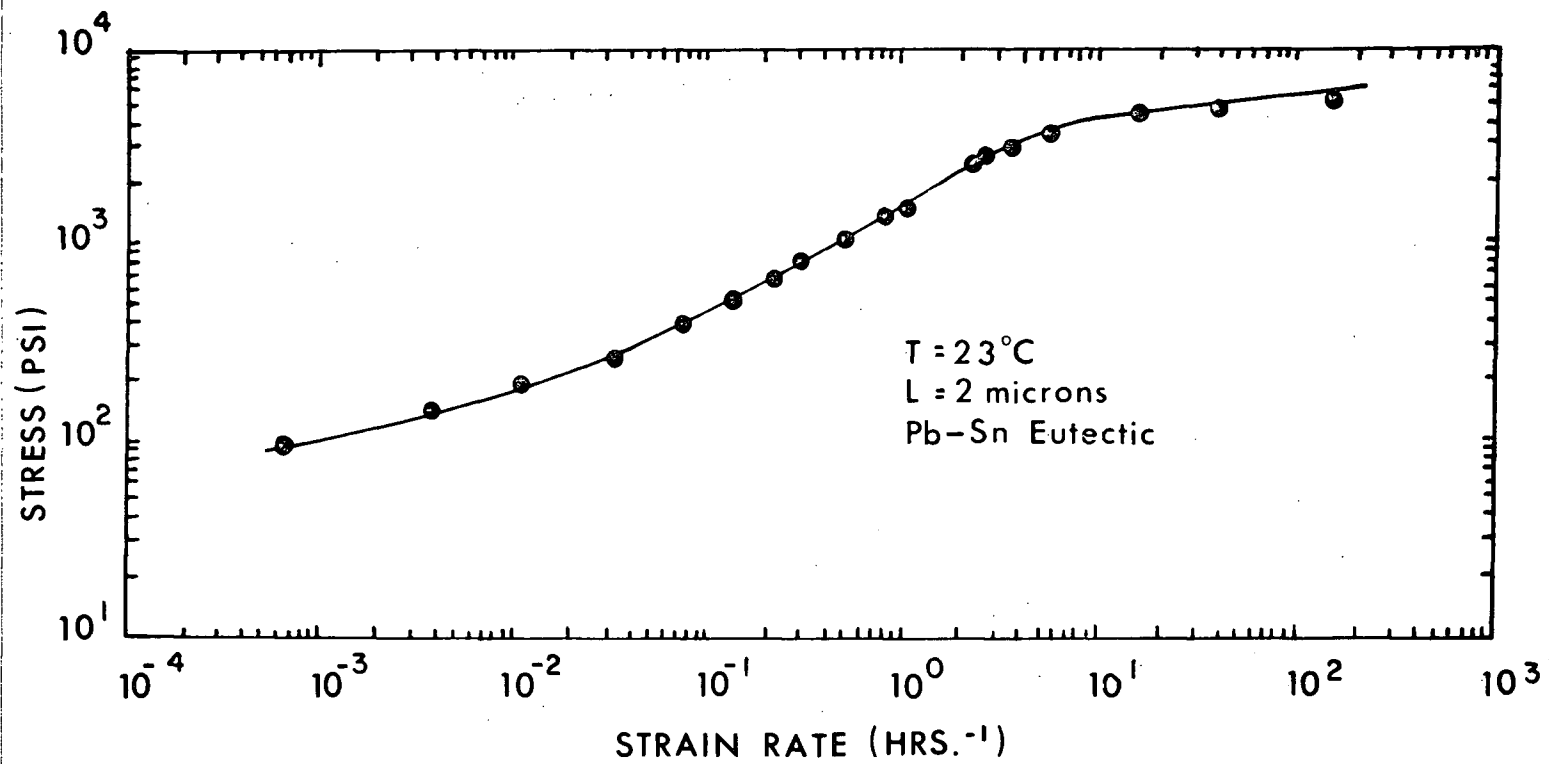


Figure 4. Log stress versus log strain curve (SGS, 2 microns).

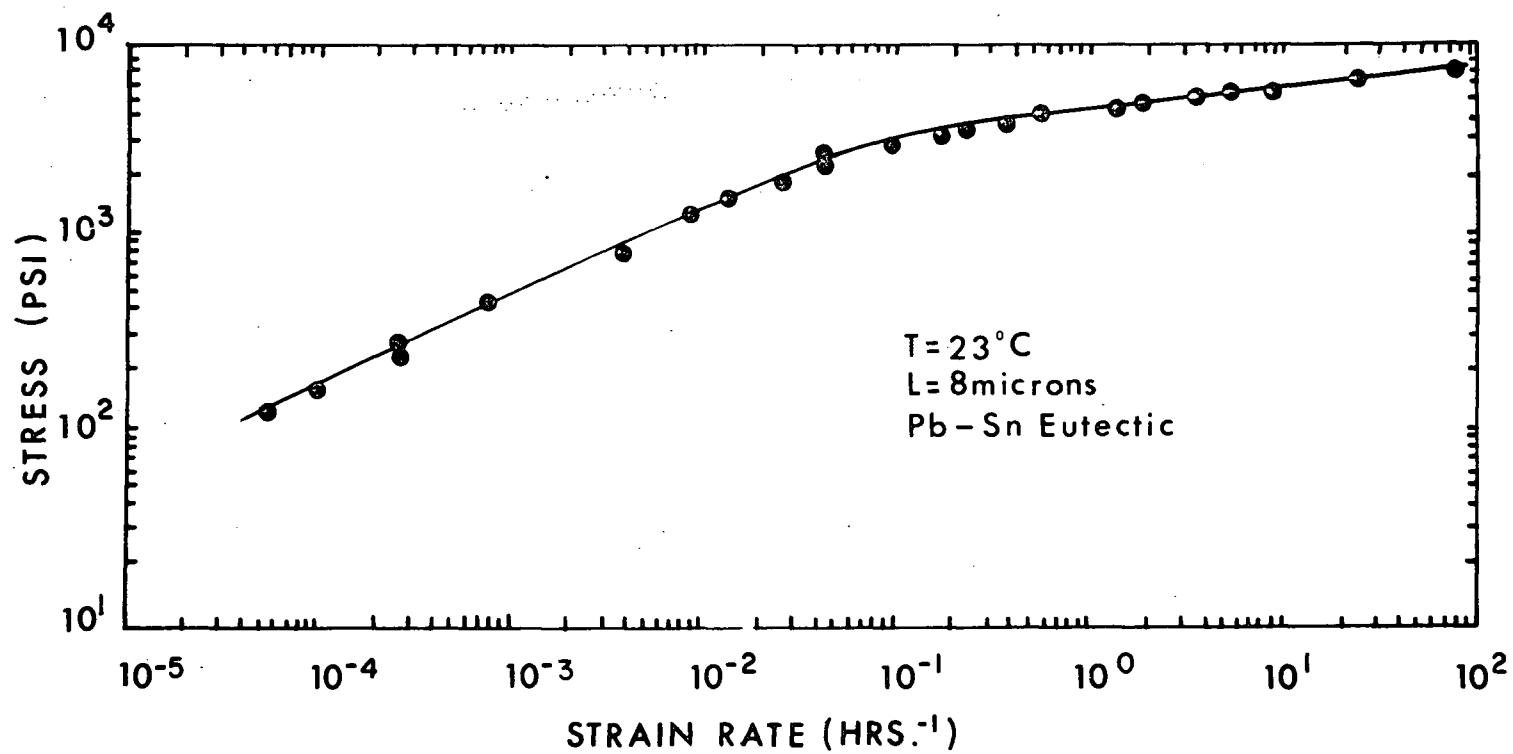


Figure 5. Log stress versus log strain rate curve (LGS, 8 microns).

The plot for the 2 micron grain size is similar to that determined by Zehr and Backofen¹⁰. The slope, or m value, in Stage I is .33. Stage II shows a slope of .5 generally with a peak value of about .6. The slope decreases after peak m as strain rate increases and approaches .10 in stage III. The curve determined by Zehr and Backofen, and also using Cline and Alden's data, is shown in Figure 6. Other points are those determined in the present work. Even if the two sets of data were brought more closely into coincidence by moving one set of data to a slightly different strain rate, the present work shows higher stress values in stage II and lower values in stage III.

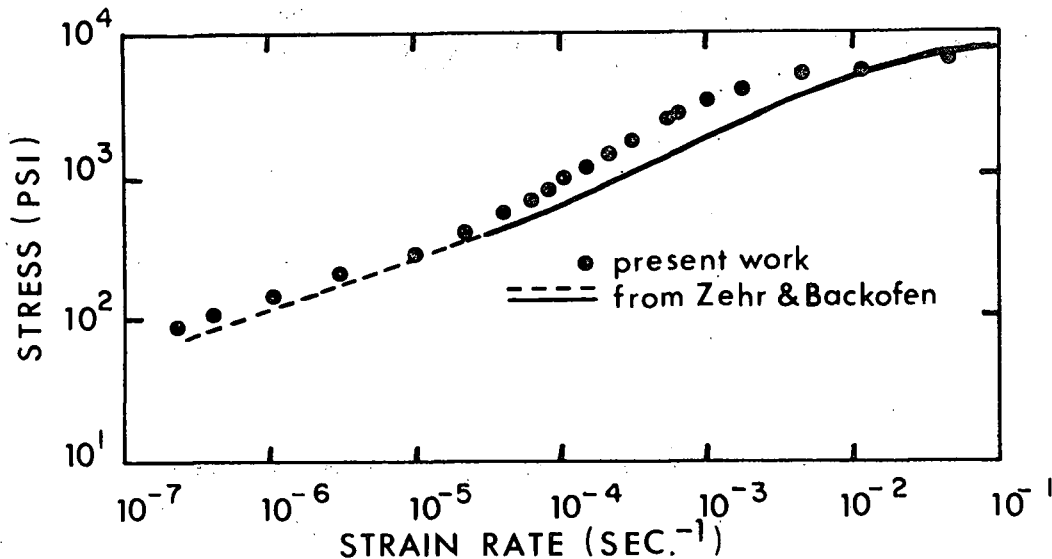


Figure 6: Comparison of the S-curve data of the present and previous work.

The plot for the 8 micron grain size shows only stages II and III. Stage II shows an m value of .5 which falls off to a stage III value of .10. A stage II-stage transition might be present but lower strain rate data would be required before it could be stated that stage I has been reached.

3.3. Creep Curves

3.3.1. Stage II Creep Curves

For specimens of both grain sizes the true strain versus time curves were straight lines. No primary creep was observed. Steady state creep was

observed from the start of each test. No necking was present during deformation. For SGS specimens, linear creep curves were observed from near 300 psi with a strain rate of $5 \times 10^{-2} \text{ hr}^{-1}$, to 2400 psi which is approximately the stress at maximum m . Figures 7 and 8 show curves near the extremes of this stress range. Another curve is shown in Figure 9. Above this stress range m decreased as stage III was approached. Below 300 psi, stage I behaviour was found. More curves typical of stage II are shown in Appendix II, Figures a to c.

Creep tests on LGS specimens did not extend to low enough strain rates to determine a transition stress and strain rate between stages I and II. Straight line creep curves were evident up to a stress of 1500 psi where m began to decrease. Examples are shown in Figure 10 and Appendix II, Figures d and e.

3.3.2. Stage I Creep Curves

Creep tests carried out in the stress range associated with stage I showed a creep curve with ever decreasing strain rate. At a stress of 97 psi, a SGS specimen was extended to a true strain of .446 after 696.5 hours. Figure 11 shows this creep curve. LGS creep tests at low stresses were only taken to a few percent elongation and only the creep rate rather than the creep curve shape was determined. Figures f, g, and h in Appendix II show more SGS creep curves for stage I.

3.3.3. Stage II -Stage III Transition Creep Curves

As strain rate is increased above that associated with peak m , the creep curves change from the straight lines of stage II. Creep curves in this transition range all had an initial linear region but the curve increased in slope, as in tertiary creep, after a strain of a few percent. All specimens,

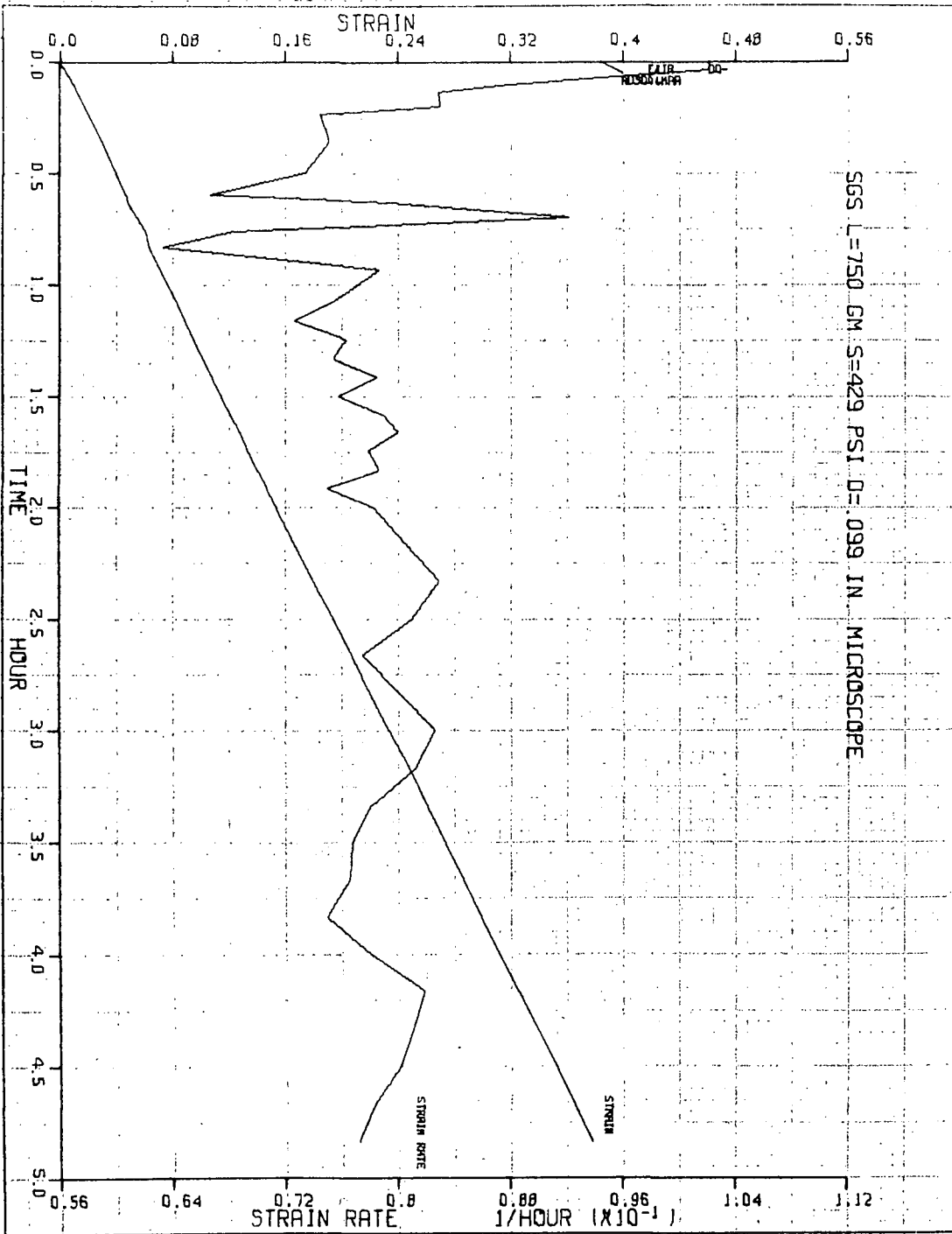


Figure 7. Stage II creep curve (SGS), 429 psi.

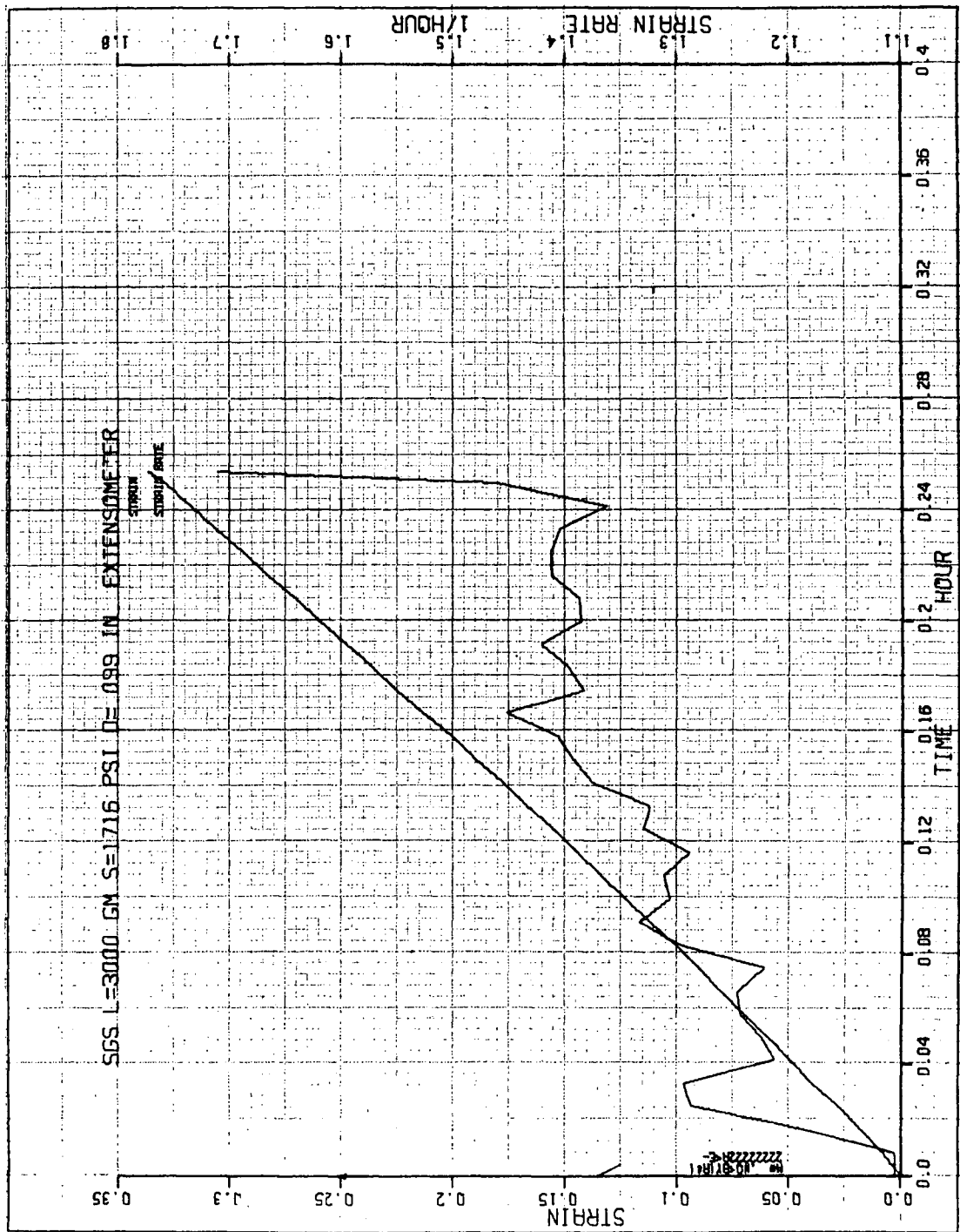


Figure 8. Stage II creep curve (SGS) 1716 psi.

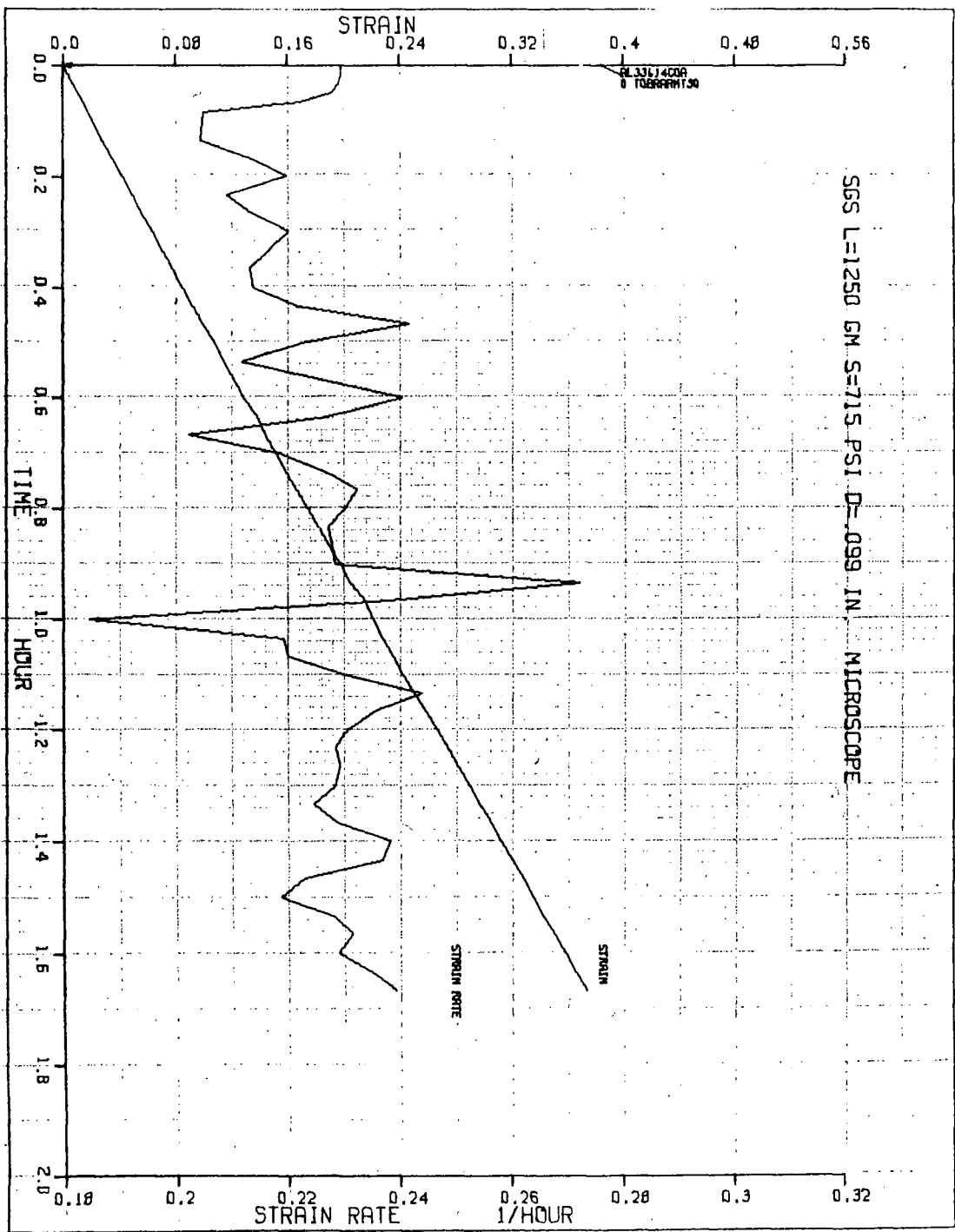


Figure 9. Stage II creep curve (SGS), 715 psi.

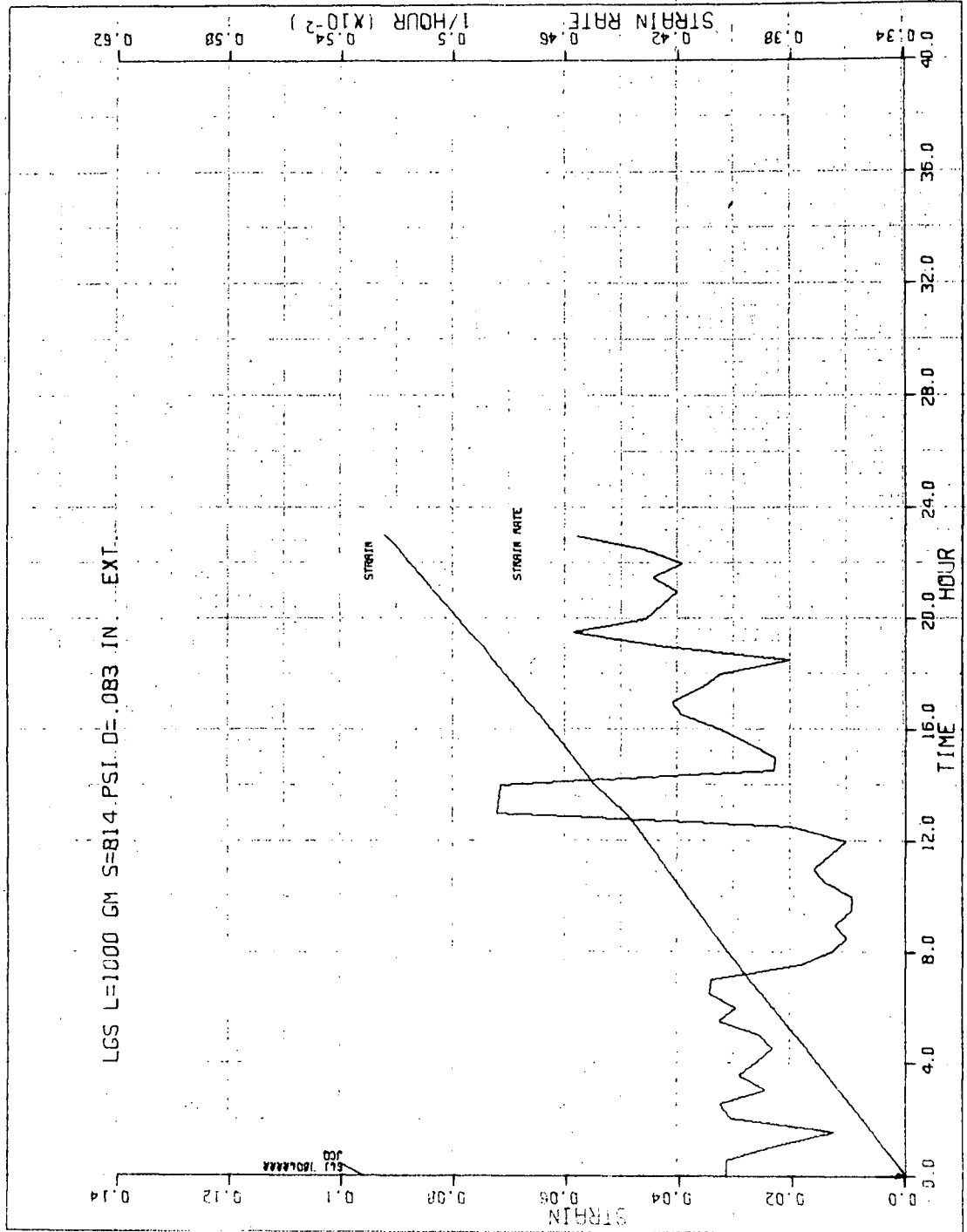


Figure 10. Stage II creep curve (LGS), 814 psi.

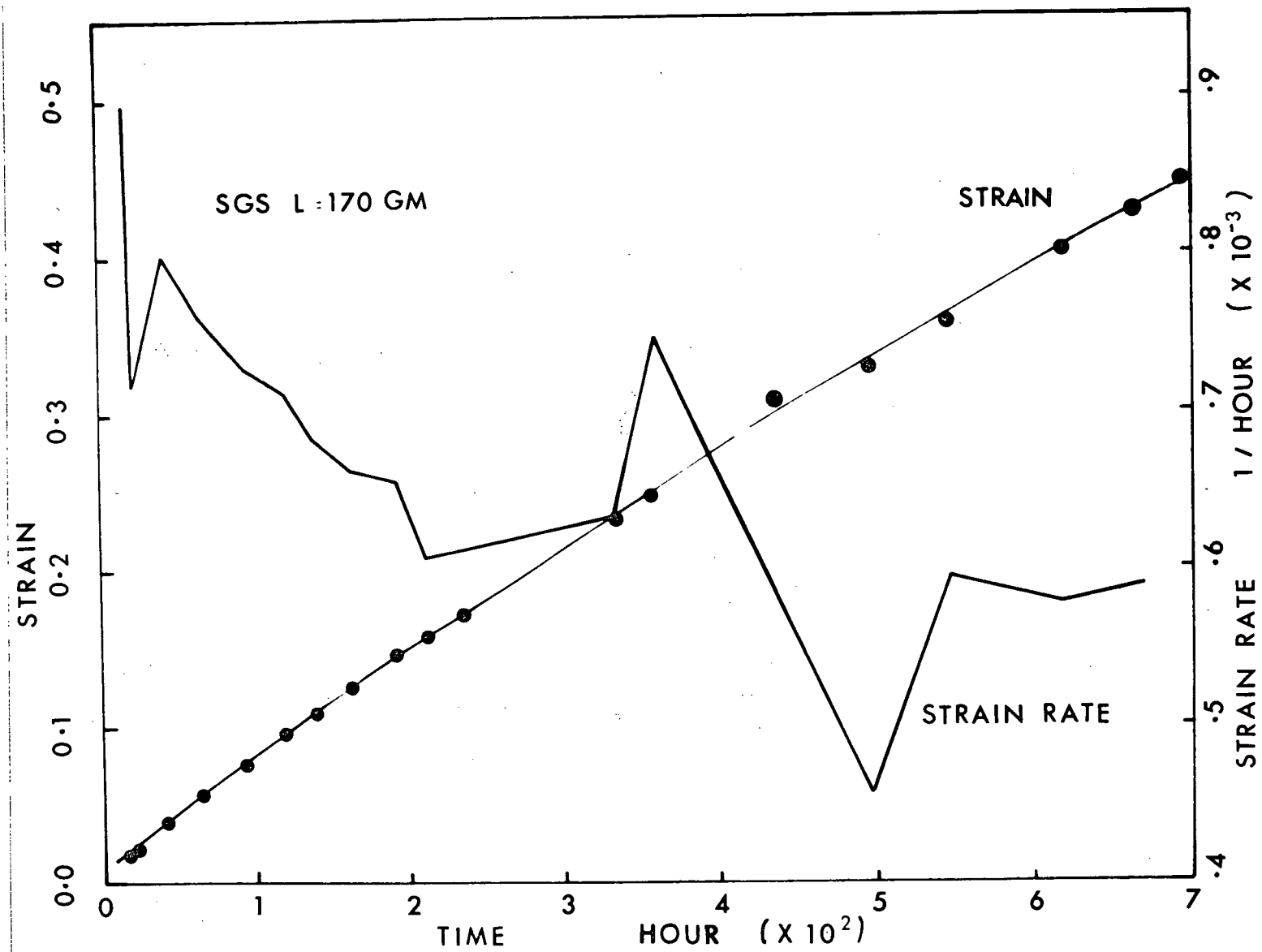


Figure 11. Stage I creep curve (SGS), 97 psi.

in this region of decreasing m , exhibited neck formation and failure occurred at less than .50 true strain. The transition region continued to 5000 psi, in the LGS, where m approached a constant value of .10. High strain rates prevented the determination of the end of the stage II - stage III transition. Figures 12 and 13 show creep curves for the stage II - stage II transition for both grain sizes. More plots are shown in Figures i to s in Appendix II.

3.3.4. Stage III Creep Curves

Creep plots in this stress range showed 3-stage creep curves. There was an initial transient. Primary creep was followed by steady state or secondary creep as strain increased. Fracture generally occurred at lower and lower strains as the creep stress was increased. Creep curves were obtained only for LGS specimens because the very high strain rates involved to attain stage III behaviour in the SGS material made recording of the deformation impossible with the experimental equipment used. Figures 14, 15 and 16 demonstrate creep curves, obtained from LGS specimens, over a range of stress. Two more curves are shown in Figures t and u in Appendix II. Figure 17 is a plot of the strain at which steady state creep appears versus the testing stress for the LGS material. The beginning of stage III is thus near 2500 psi.

3.4. Incremental Loading and Unloading

Incremental loading and unloading tests were made during creep tests on specimens of both grain sizes in stage II and III. In stage II, where creep curves are linear, increasing and decreasing the load results in an abrupt transition to linear curves of increasing or decreasing slope. Figure 18 is an example of incremental loading of a SGS specimen. The short strain rate peak,

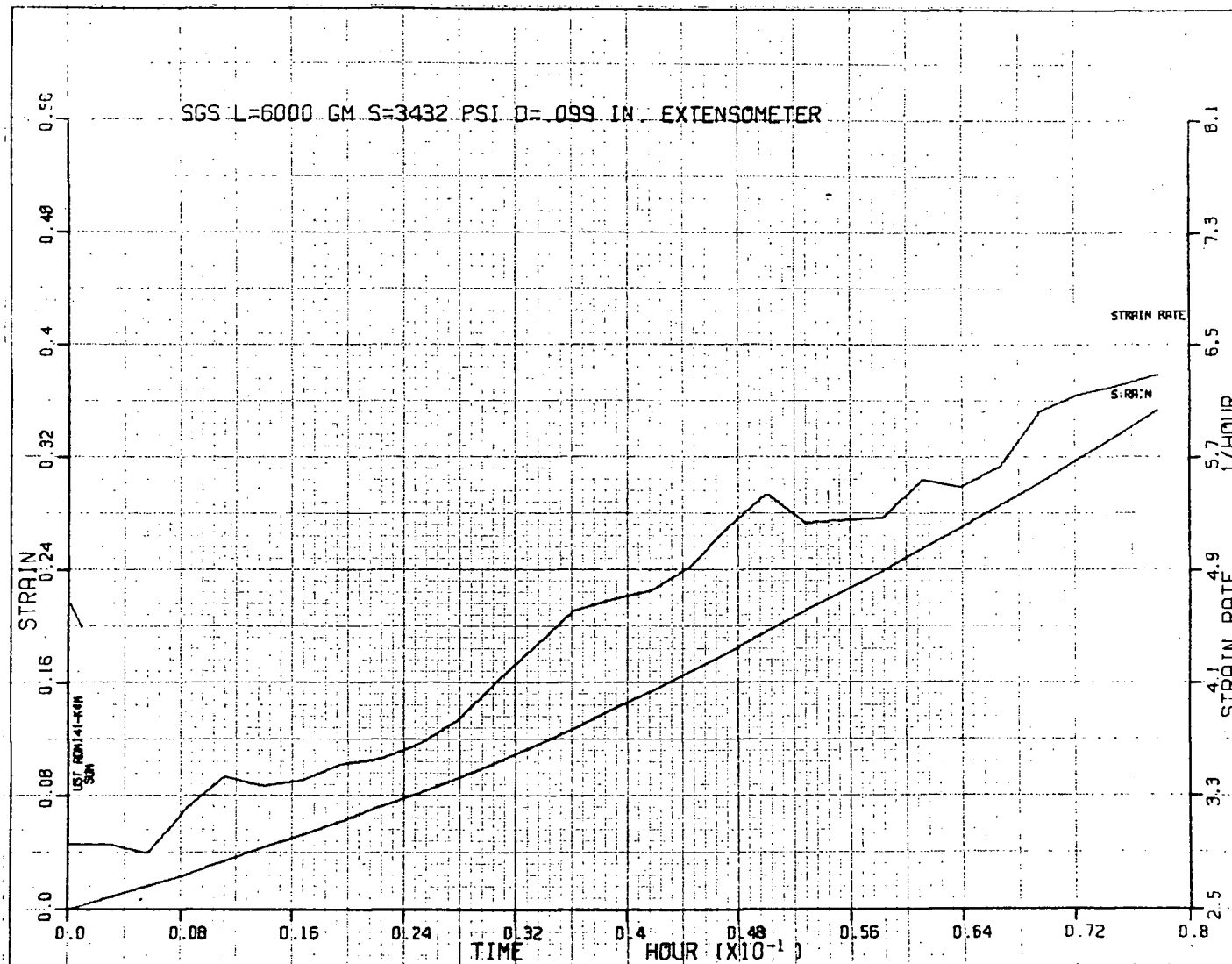


Figure 12. Creep curve in stage II -- stage II transition (SGS), 3432 psi.

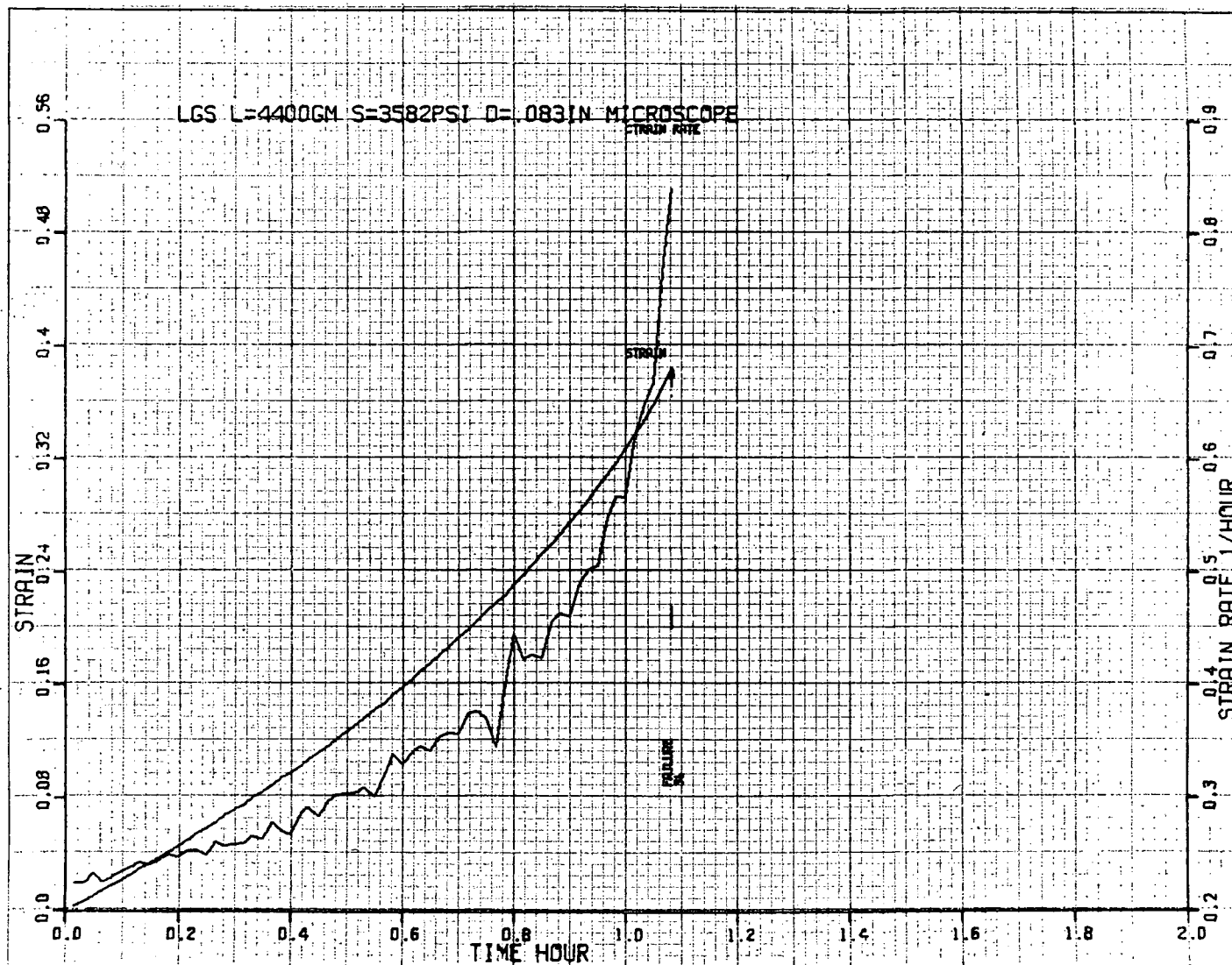


Figure 13. Creep curve in stage II - stage III transition (LGS), 3582 psi.

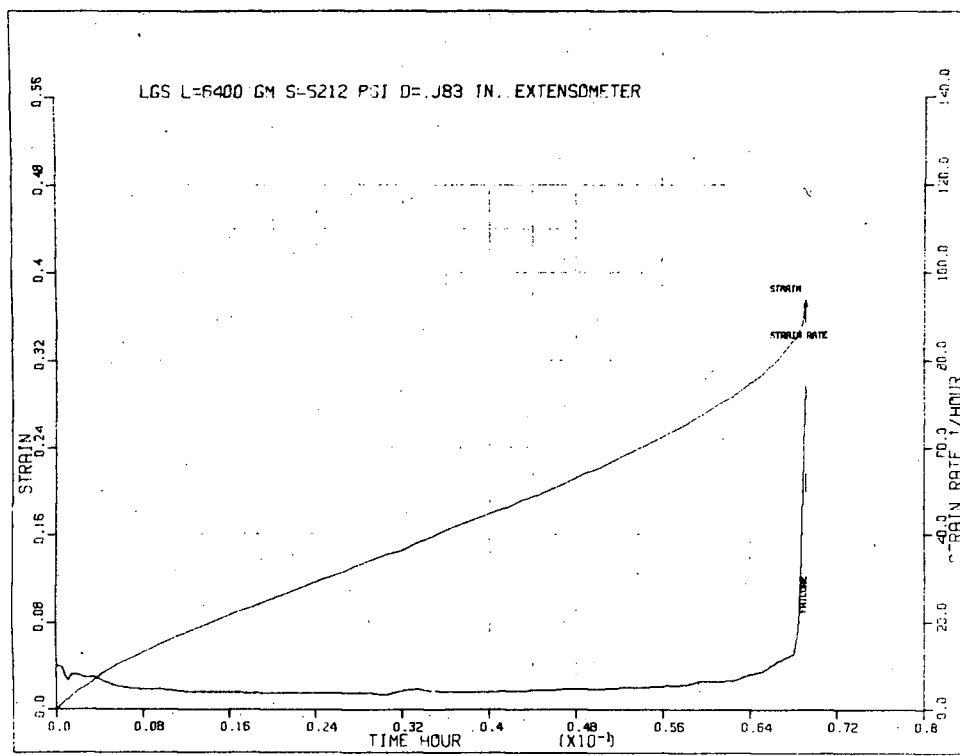


Figure 14. Stage III creep curve (5212 psi)

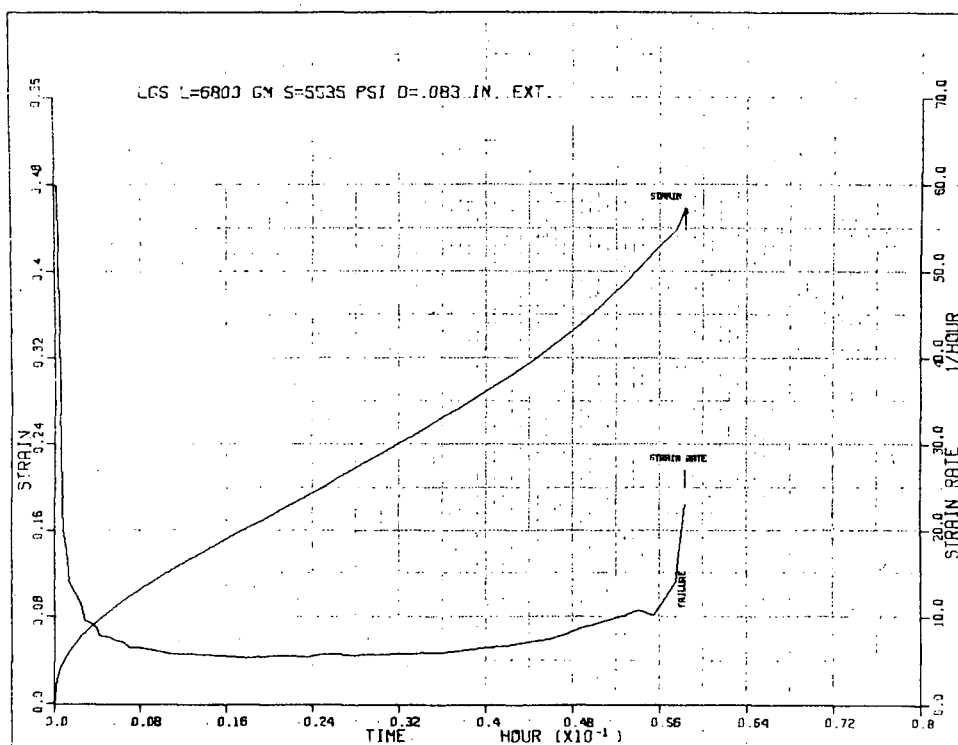


Figure 15. Stage III creep curve (5535 psi)

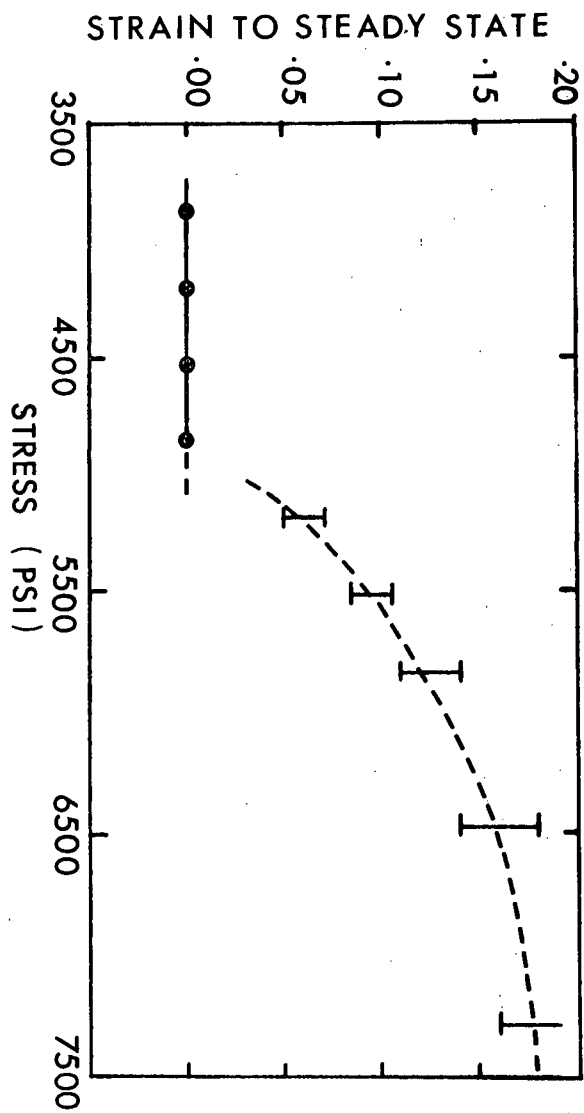


Figure 17. Strain required to reach steady state versus creep stress.

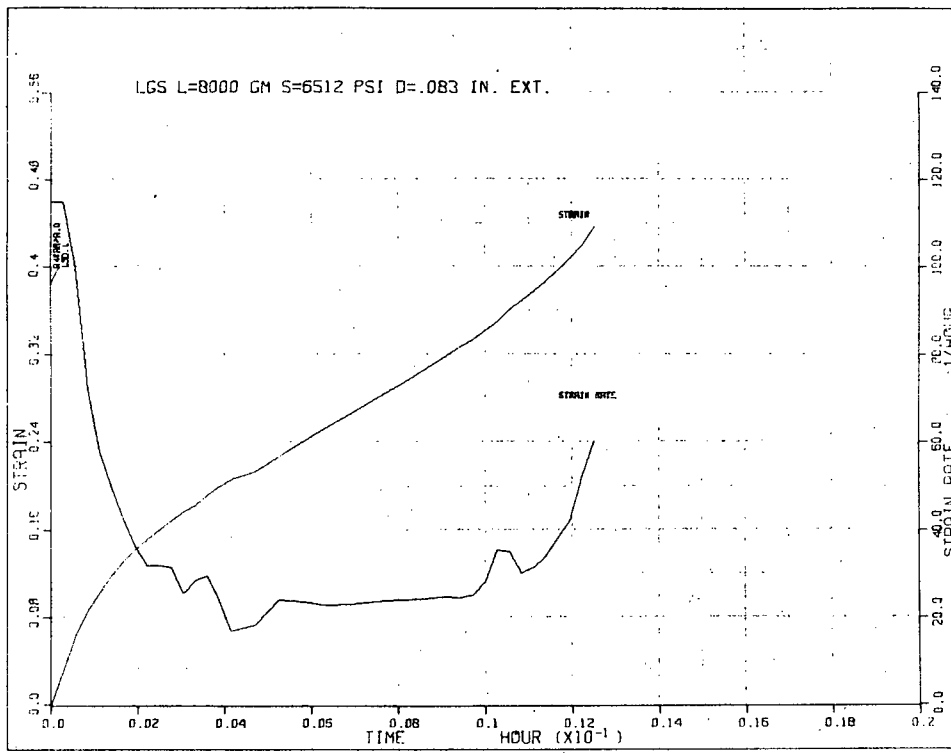


Figure 16. Stage III creep curve (6512 psi).

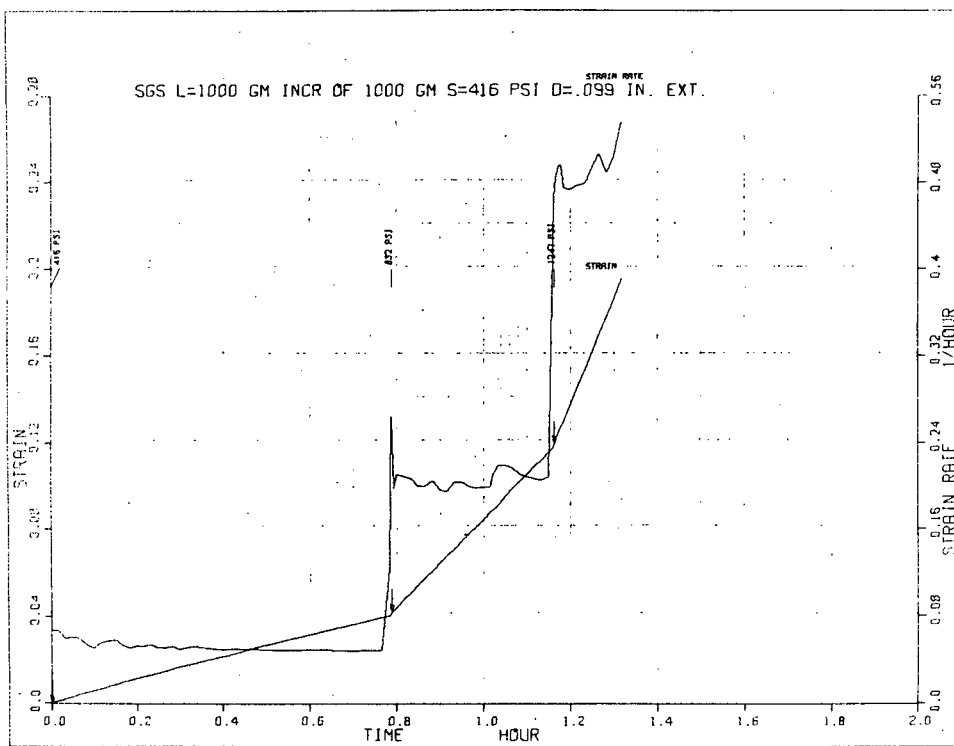


Figure 18. Incremental loading during superplastic creep.

when the stress reaches 832 psi, is due to an error in one reading exactly at transition. Another incremental loading example is shown in Figure v Appendix II. Curves have the same slope at all stresses in stage II, during incremental loading, as when they are initially loaded to that stress. Strain rate is independent of prior history in stage II.

Incremental loading during primary creep in stage III results in a change in the initial transient. The slope of the curve is instantly increased and a transient remains to a higher strain than would have occurred at the lower stress.

Figure 19 shows the result of increasing the load during steady state creep in stage III. Here, a transient reappears. Figure 20 shows the immediate transition to steady state creep when the load is decreased during primary creep. This result is also shown in Figure w, Appendix II.

The purpose of these tests was to compare the behaviour of a superplastic material, during loading and unloading, to the behaviour of non-superplastic materials under similar testing conditions.

3.5. Strain After-Effects

Specimens deforming in stage II and stage III were unloaded. These specimens were then continuously measured with an extensometer to look for strain relaxation. At no time was there any sign of contraction during stage II. An example of this result is shown in Figure 21. Results of tests on LGS samples in stage III were not conclusive but always suggested some strain relaxation. Relaxations of .003 to .004 inches were found on a gauge length of .500 inches after times of 45 minutes to 60 minutes after strains of .10

to .30. The return of primary creep after recovery was looked for. Once again the effect is small as shown by Figure 22 after 5 minutes recovery time. It may be that recovery rates are too slow at room temperature. Recovery at higher temperatures forced the removal of the extensometer and specimen distortion occurred. These problems once again lead to inconclusive results.

4. DISCUSSION

Creep studies of superplastic materials have seldom been made. Previous work on lead, tin and the lead-tin eutectic³³⁻³⁵ has not involved stresses, strain rates and grain sizes necessary to obtain superplastic behaviour. Packer, Johnson and Sherby³⁸ used constant stress creep tests in their study of eutectic Zn-Al and state that they found negligible strain hardening during superplastic creep and that the creep rate remained constant under constant stress and temperature. Zehr and Backofen¹⁰ used a creep test to obtain a low strain rate value on an S-curve for Pb-Sn. Chaudhari³² has also done some creep work. The present study has been the only one specifically designed to gain more insight into the superplastic phenomena through the study of creep curve details over a wide stress range. Discussion will cover mainly the merits of recently suggested mechanisms of superplasticity, considered in view of new creep results and other consistently reported observations.

4.1. Stage III

Deformation in stage III is not superplastic. It is similar to the creep of coarse grained materials where deformation is by recovery creep. This conclusion follows from the current observations of primary creep, a

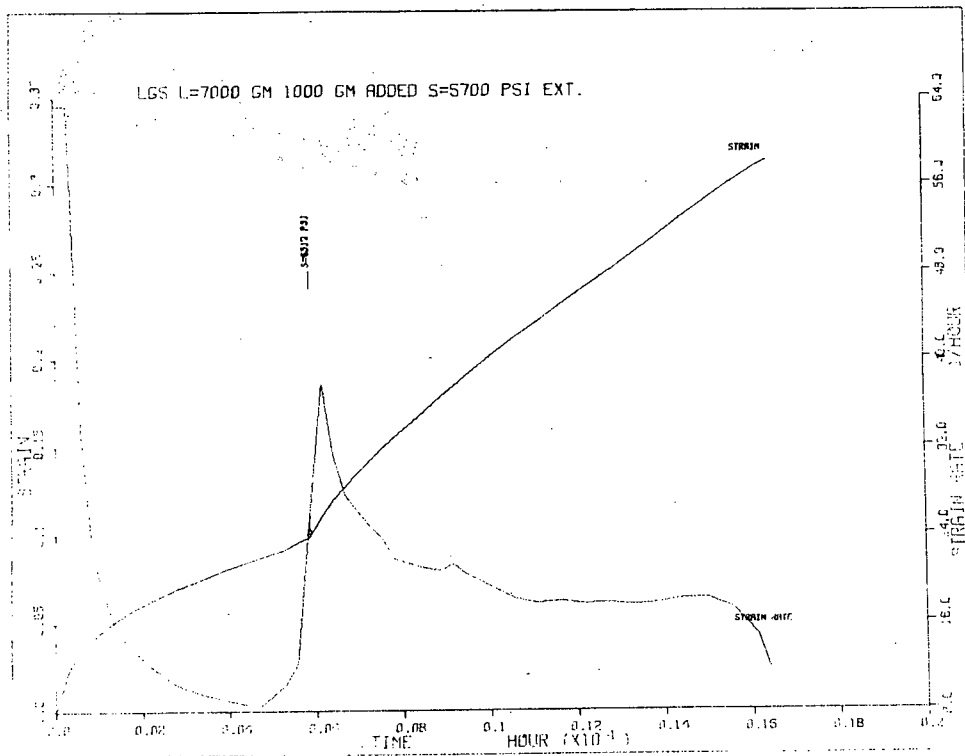


Figure 19. Return of an initial transient with incremental loading in stage III.

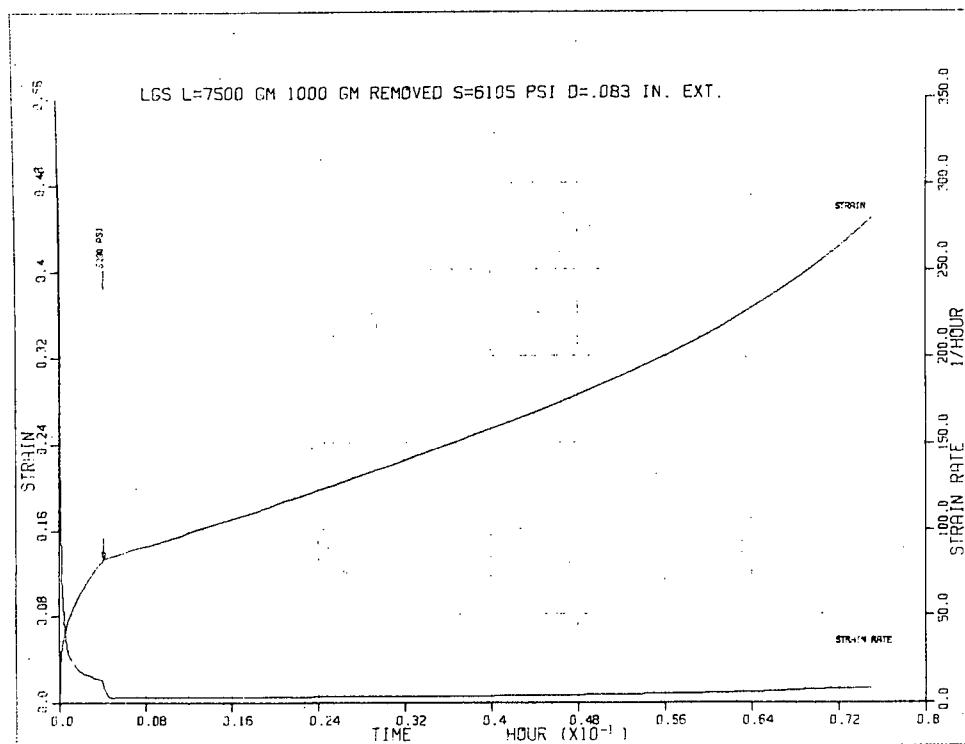


Figure 20. Transition to steady state with unloading in stage III.

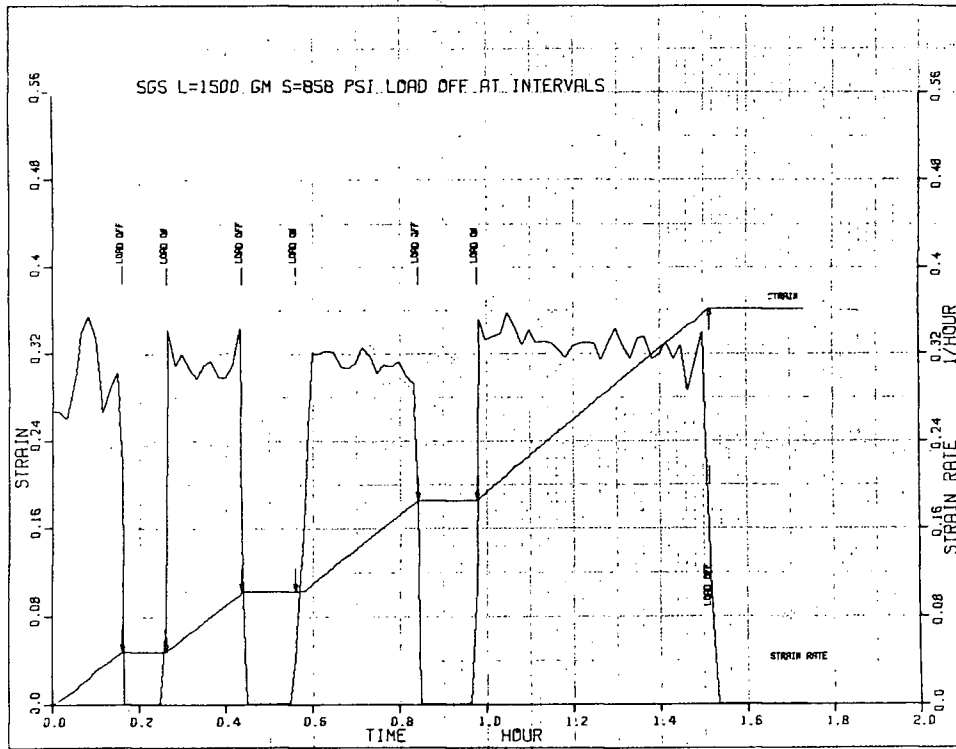


Figure 21. Strain relaxation study in stage II.

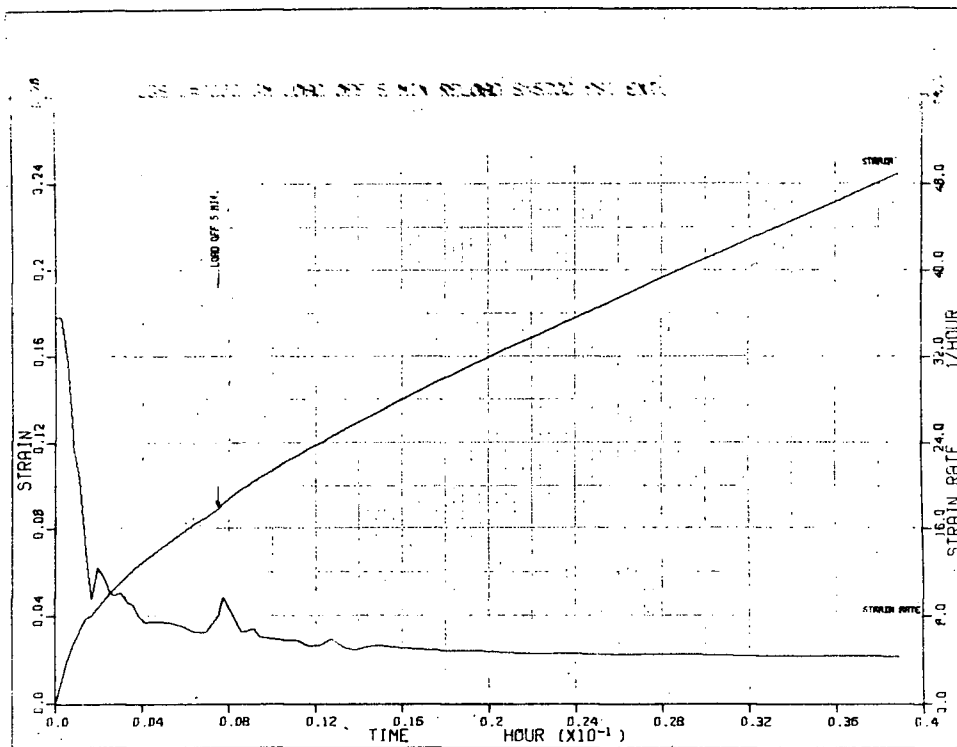


Figure 22. Reloading after recovery in stage III.

3-stage creep curve and a low m value near .10. A dislocation substructure is also present after stage III creep^{1,6,7,39}, as in the creep of coarse grained materials³⁷. Results (Figure 21) also seem to show the return of an initial transient after recovery. However, significantly larger transients were not seen at larger recovery times. A strain after-effect, whereby the specimens shortened slightly when the load was removed after elongation, has also been observed in coarse grained materials³⁷ after recovery creep. Present results seem to show that this did occur after stage III deformation. Necking was associated with tertiary creep.

Recovery creep theories involve a general equation for steady state strain rate,

$$\dot{\epsilon} = r/h \quad (3)$$

where r is the recovery rate, $d\sigma/dt$, and h is strain hardening $dh/d\epsilon$.

Strain hardening is associated with an increase in dislocation density (ρ) while recovery represents a decrease. Primary creep results if the initial recovery rate is smaller than the hardening rate. The value of r in an annealed specimen is close to zero. Steady state creep represents a balance between hardening and recovery. Such a balance is expected only after some increase in dislocation density, relative to the annealed condition, which occurs during primary creep.

A modern theory for stage III is that of McLean⁴⁰. Deformation at high temperatures involves the behaviour of a three-dimensional dislocation network. Three important aspects of this behaviour are the temperature insensitivity of the flow stress of a given network, the network's tendency to coarsen on heating which corresponds to a decrease in ρ and its refinement

on straining which corresponds to an increase.

McLean shows that the recovery rate, r , varies with stress by

$$r \propto \sigma^3 \quad (4)$$

The recovery process involves diffusion controlled dislocation climb and migration of jogs in screws. Therefore, if D is the diffusion coefficient

$$r \propto \sigma^3 D \quad (5)$$

Plastic deformation refines the dislocation network. During deformation, moving dislocations are held up at points where the network is fine and bow out to increase the average dislocation density. Multiple slip permits network geometry to remain constant as the meshes become smaller. The strain hardening coefficient $h = \partial\sigma/\partial\epsilon$ is a measure of the refining action. If expression for r from eqn.(5) and h from the empirical relationship $h \propto \sigma^{-3/2}$ are used in eqn(3) the result is

$$\epsilon = BD\sigma^{4.5} \quad (6)$$

or if $K = (1/BD)^{1/4.5}$

$$\sigma = K\epsilon^{.22} \quad (7)$$

which is the same as equation (1) with $m = .22$. This value of m is not quite as low as that found experimentally. Theories of this type are, of course, rather speculative and evidently approximate in nature. It is not known to what extent the physical model of McLean corresponds to the detailed deformation and recovery processes in stage III.

4.2. Stage II-Stage III Transition

In the stage II-stage III transition, on increasing strain rate, m falls from a maximum to a small essentially constant value associated with stage III. The transition strain rate range was from $2 \times 10^{-2} \text{ hr.}^{-1}$ to 2 hr.^{-1} for the 8 micron grain size and above 2.5 hr.^{-1} for the 2 micron grain size. The high strain rates involved prevented differentiation between the end of the transition range and the start of stage III in the small grain size specimens. Creep curves in the transition region are convex upward (tertiary creep) (Figures 12 and 13). There is no primary creep. Failure occurs at strains of less than .50 and failure occurs at a neck. Chaudhari⁴¹ may have explained this result mathematically. Differentiation of equation (1) leads to

$$\frac{d\dot{\epsilon}}{\dot{\epsilon}} = \frac{1}{m} \left[\frac{d\sigma}{\sigma} - \log \left(\frac{\sigma}{K} \right) \frac{dm}{m} \right] \quad (2)$$

The effect of a large m value is to decrease the tendency for a neck to grow. Conversely, an increase in the bracketed term increases the sensitivity to necking. If m is decreasing with increasing strain rate, as it is in the transition range, dm is negative and the second term will be added to the first. The bracketed term becomes larger and sensitivity to necking is more pronounced. Observations of neck formation and growth after only a few percent strain were made during the present work (Figures 12 and 13). Previous observations¹⁶ of large superplastic elongations using initial strain rates in this region were made with Instron tensile machines. These machines have a constant cross head speed and the strain rate imposed on a specimen is continuously decreasing. The effect of a

decreasing strain rate in the transition range is to give a rising n value as testing proceeds.

A convex upward creep curve has previously been reported in the literature³⁶ but no comment or explanation was attempted. Constant stress creep tests were performed on a number of pure tin specimens. Four different grain sizes were used but only the finest, 37 microns, exhibited this behaviour. Others showed primary creep. Figure 23 shows a logarithmic plot of stress versus strain rate using Breen and Weertman's creep rate data for the smallest grain size. This curve is somewhat comparable to that of Alden⁶ and differences may be due to grain growth and the fact that Alden's curve was obtained using an Instron tensile machine. n varies from .3 to .12.

The increase in n with decreasing strain rate is due to a slow increase in sub-grain size with decreasing strain rate⁴². Stage II is reached when sub-grain size has reached the grain size^{1,13}. As this condition is approached, accommodation for GBS by slip becomes easier and n increases to its maximum value. The stage III - stage II transition is associated with increased amounts of GBS⁵.

Superplasticity may actually be possible in larger grained materials if, at low enough strain rates, the sub grain size approaches the grain size. Creep tests by Gifkins⁴³ may be indicative of this. The grain size of extruded Pb-2.45 wt% thallium was 100 microns. Stresses of 300,500,1000,1500, and 2000 psi were used on creep specimens.

These creep results are plotted in Figure 24. The n value increases from .15 to .45. Microstructural observations showed that slip lines became less regular and more widely spread as the stress was decreased and at the lowest strain rates deformation proceeded by "boundary micro-flow" and grains were undeformed. At 500 psi elongation to failure was 208 %. Similar observations were made

by Wood et al⁴⁴ on aluminum with a grain size of 100 to 200 microns. Slip was prominent during deformation at lower temperatures and higher rates of strain. As the temperature was increased or the strain rate decreased, slip lines gradually vanished and the elements of the associated substructure showed an increase in size. This left a coarse substructure which increased in size with a further increase in temperature or decrease in strain rate until it was the size of the grain itself. This coincided with the onset of prominent "boundary micro flow" or GBS. They found that lattice structure was unchanged and no strain hardening occurred during deformation.

The observations of Wood et al and Gifkins seem to be very similar to the observations made on fine grained superplastic materials where GBS becomes more dominant as the strain rate is decreased from that of stage III¹³.

4.3. Stage II

The new observations associated with stage II are that the creep curves are linear and that there are no unloading transients. The linear creep curves are shown in Figures 8,11. There are no signs of primary or tertiary creep, only steady state. The results of unloading tests are shown in Figure 21. No contractions due to recovery has occurred. These results show that recovery theories, which may be valid for normal creep, and stage III are unsatisfactory for superplastic creep. Alden⁴⁵ has demonstrated that many proposed models for superplasticity are really models based on recovery creep and are thus unacceptable. An internal stress model³² which incorporates an accumulation of dislocations near the grain boundary seems to be unacceptable because dislocations are not seen during superplastic deformation even when specimens are quenched under load¹.

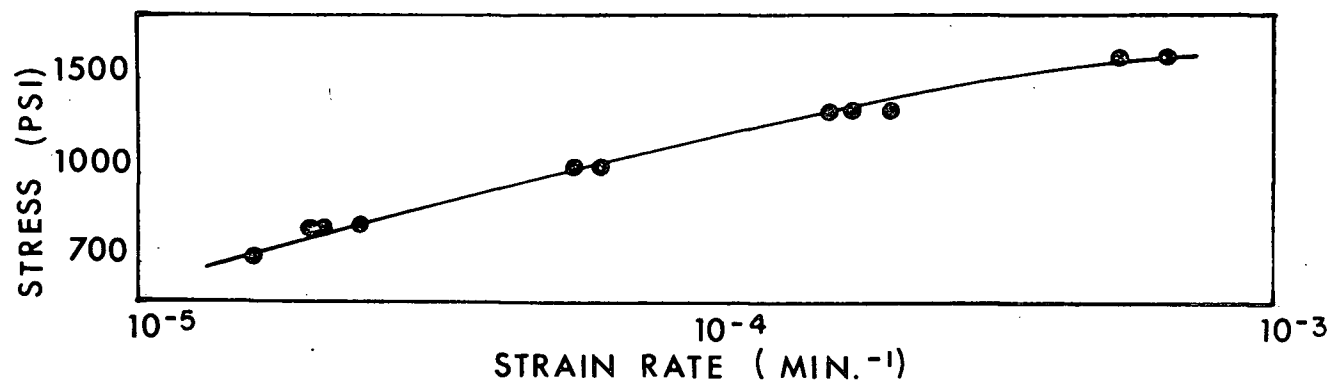


Figure 23. Log stress versus log strain rate relationship for pure tin (37μ).

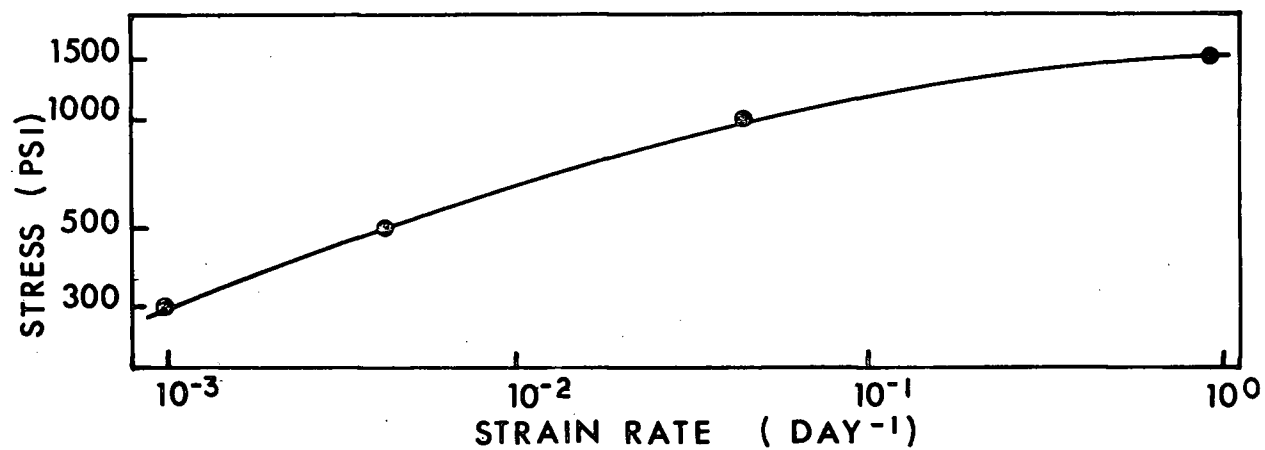


Figure 24. Log stress versus log strain rate relationship for Pb-2.45 wt.% thallium (100μ).

Also, the low temperature yield stress is unchanged after stage II deformation¹³. If dislocations are accumulated during creep, this yield stress should increase. Mechanisms and accommodation processes which would show no transients are those which do not involve a structural change. Grain boundary sliding with some special accommodation processes, Nabarro-Herring or Coble creep and grain boundary migration are examples.

Grain boundary migration, in association with GBS, has been observed in superplastic materials^{46,47}. Opposition to the idea that migration is rate-controlling is based on doubt that migration can be effective when many phase boundaries are present in two phase systems. At the same time, it must be considered that if there are equal amounts of two phases, each phase might still be in contact with 50 % of the like phase. Thus there is a reasonable chance for migration to be an effective means of accommodation for GBS in a superplastic material. With only one phase present, dilute alloy systems do not, of course, present this problem.

Grain elongation should result during diffusional creep. This is not observed in stage II¹⁰ but Zehr and Bachofen's explanation is that elongated grains will experience a shape relaxation during straining through direct migration and recrystallization. They claim that the presence of striated bands on a 2 micron Pb-Sn eutectic specimen pulled at 3.3×10^{-5} sec.⁻¹ supports diffusional creep. This strain rate is very near the transition to stage I. Similar striations have been observed in Cd-5 % Pb⁴⁷ over strain rates associated with stages I and II. Donaldson⁴⁷ suggests that striations may indicate that boundary sliding occurs on preferred crystallographic planes. The test of this is to correlate grain orientation and the planar orientation of the slipped boundaries with striation spacing.

Narrow striation spacing would indicate large mis-orientation. The absence of striations would indicate that the sliding plane is a preferred plane.

In a Mg-Al alloy, the strain contribution of grain boundary sliding in stage II reached 65 %¹. Alden suggests that the grain boundaries may act as "perfect" sinks and that sliding is rate-controlled by diffusion. This model demands that the absorption rate by boundaries of dislocations generated at triple lines be so high that it is not rate controlling. Fast recovery rates in superplastic materials¹³ support this but little or no climb can be involved or this becomes a recovery creep model. Absorption may be enhanced by GBS by the attraction force between sliding boundaries and dislocations¹. The rate of sliding is determined by the effective viscosity of the boundary. The boundaries are rough and the sliding rate is determined by diffusion around these rough areas. The scale of roughness will usually increase with grain size. The model predicts the strain rate semi quantitatively in agreement with observed effects of stress, grain size, and temperature.

4.4. Stage I

Stage I, as shown in Figure 11, is similar to stage II in that there are no transients similar to those found in stage III. The creep curve is not linear, however. There is a definite decrease in strain rate with time. This decreasing strain rate is not believed to be in any way representative of a recovery creep model where a decreasing creep rate is found during primary creep.

Stage I may represent a change in the rate controlling process for GBS from diffusion around bumps on boundaries to slip at triple lines. If dislocations are emitted from a source, proceed through a material without barriers and are then absorbed at a "perfect" sink, no strain hardening will result. If the

sources of dislocations are the edges of sliding grains, and the sinks are grain boundaries, Alden³⁰ suggests that strain rate will depend on stress to the power 2 to 3. The slope depends on whether accommodation dislocations move on a few slip planes or throughout the grain volume. A linear array is expected in alloys with a low stacking fault energy such as Fe-Ni-Cr and m should be .5. Motion normal to the slip plane is easier through cross slip in high stacking fault energy material and the slope should be .33 as was observed.

Lee¹ found the behaviour in stage I to be a combined effect of grain deformation and deformation across transverse grain boundaries, accounting roughly for 1/3 and 2/3 of the total deformation, respectively. The latter consisted, at least in part, of GBS but whether the remaining fraction was due to GBS or Coble creep could not be determined.

Several experimental observations suggest that diffusional creep may contribute to deformation in stage I. These are grain elongation^{7,28}, striations¹⁰ and denuded zones²⁹, and creep curves of decreasing slope.

Creep curves of decreasing slope could occur by the self-extinguishing nature of diffusional creep. A theoretical analysis of N-H and Coble creep has been made and details are shown in Appendix III. Figure 25 shows the shape of creep curves expected for pure N-H and Coble creep. A stage I experimental curve is also shown and all are put on a time scale representing the fraction of total time to reach .40 true strain. Times involved for .40 strain are .87 hrs. for Coble creep and 5.39×10^5 hrs. for N-H creep. The experimental curve represents 700 hours and could be partially representative of some combination of N-H and Coble creep.

It has been reported that there is no grain elongation in the Pb-Sn eutectic¹⁰ in stage I. There is grain growth during deformation¹⁹ and also grain strain. Grain rotation has been observed¹⁶. Lack of grain elongation might not

exclude diffusional creep as an important part of the deformation mechanism of stage I. A grain may elongate, by diffusion, parallel to the tensile axis. Grain boundary migration could account for the return of an equiaxed shape and an increased grain size. Grain rotation would change the tensile axis and permit elongation in all directions. If grain growth does not involve diffusional creep, grain strain would not be expected. Lee¹ measured the travel of two marker wholly within a grain. In stage III no movement was found. In stage II this was equal to .21 of the total strain and in stage I this increased to .30. Growth of one grain at the expense of another would not contribute to an internal travel of markers but only to the grain volume. Grain growth by any means, however, could result in a creep curve of decreasing slope because the strain rate does decrease with increasing grain size.

Stage I deformation involves GBS and probably some combination of N-H and Coble creep.

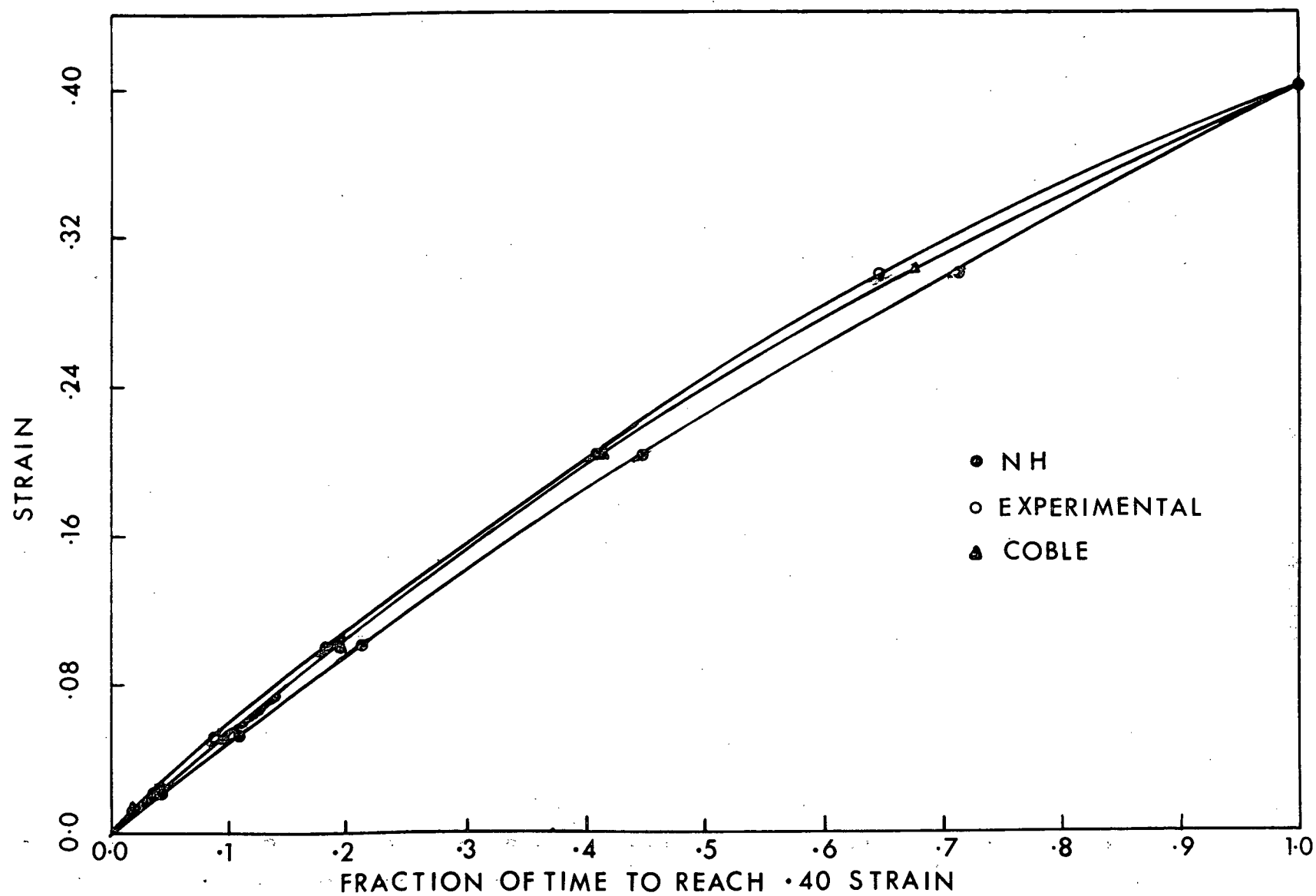


Figure 25. Experimental, theoretical N-H and theoretical Coble creep curves (97 psi).

5. SUMMARY AND CONCLUSIONS

In the superplastic range, materials display unusual creep properties. Strain rate is dependent on grain size and insensitive to stress. Creep curves are linear with no initial or final transients. A material is considered "superplastic" if superplastic properties are observed at experimentally reasonable strain rates. There is evidence that superplastic properties may occur at low enough strain rates in "normal" materials. Conversely, a "superplastic" material may display normal creep properties at sufficiently high strain rates.

In stage II, a linear creep curve suggests that the deformation mechanism accounting for superplastic behaviour must be one which involves no significant structural change. Creep curves in stage II show no transients, after loading or unloading and the strain rate, at any stress in the superplastic range, is independent of prior superplastic deformation history. Prior evidence indicates that most of the deformation in stage II is accomplished by grain boundary sliding. There must be accommodation for grain boundary sliding to operate. Accommodation could involve one or more of grain boundary migration, diffusion, or slip at triple points. The m value for stage II in the lead-tin eutectic is near .5 and has a maximum value near .6.

At low strain rates creep curves show an ever decreasing slope. this could be due to diffusion or grain growth. GBS occurs in stage I, but is not as dominating as in stage II. Grain strain increases in stage I and is notably indicative of a diffusional process. Some combination of N-H and Coble diffusional creep is likely since the experimental creep rates are much faster than those expected for N-H creep and much slower than could be

attributed to Coble creep. The rate controlling process is not known. Grain growth, grain rotation, grain boundary migration, and slip and triple lines may all have some effect on deformation and the resulting creep curve. The m value for stage I is .33 and is constant over the stress range studied.

In the stage II - stage II transition region, superplastic properties depend on the testing method. In a constant stress creep test tertiary creep begins, as necks propagate and grow, after only a few percent strain and failure occurs at less than .50 true strain in the lead-tin eutectic. Testing under conditions where the strain rate decreases as the test proceeds reduces the tendency to neck and elongation to failure is much greater.

SUGGESTIONS FOR FUTURE WORK

There are several lines of investigation which could extend from the present work. These include:

- (1) A determination of creep curves and creep rates over a wide stress range in stage I for several grain sizes.
- (2) A micrographic study of the variation of the contribution of grain boundary sliding and grain strain with stress over stage I. A study of grain elongation, grain boundary migration and grain rotation might prove helpful at low stresses.
- (3) A study of activation energy in stage I over a wide stress and temperature range and also into stage II.
- (4) An evaluation of factors, such as time temperature and elongation, contributing to grain growth during stage II deformation.
- (5) An investigation of elongation at various constant stresses over the stage II-stage III transition to determine if there is a relationship between elongation to failure and m .
- (6) A more careful study of the relationship between strain rate and grain size. Relationships between $1/L^2$ and $1/44.5$ have been reported in the literature 1,3,10,13,20. For these relationships to be valid, each value taken must be in stage II. Some relationships in the literature have involved a stress which is in two stages of the S-curve and are therefore invalid. The present work shows a $1/L^3$ dependence although there is some doubt in the grain sizes. A plot of valid points for Pb-5 %Cd¹³ and eutectic Pb-Sn shows a $1/L^3$ relationship. The relationships show scatter between -2.2 and -3.9 for Pb-Sn³ and -2 and -3 for a Mg-Al alloy.

APPENDIX I

Computer Programme

FORTRAN IV G. COMPILER		MAIN	03-17-69	18:31:04	PAGE 0001
0001	0	ANALYSIS OF THE CREEP TEST CURVES			PHB004
		DIMENSION TITLE(14),IND(20,20), TIME(20,20),GRAD(20,20),			PHB005
		ISTRAIN(200), TIMEX(200),RATE(200),IN(200),DIAL(20,20),XC(5),YC(5)			PHB006
0002		READ(5,8) NEXTECU			PHB007
0003	8	FORMAT(15X,13)			PHB008
0004		DO 60 I = 1,NEXTECU			PHB009
0005		READ(5,1)TITLE			PHB010
0006	1	FORMAT(14A4)			
0007		READ(5,4) SCAFAC,NSHIFT,ELNOT			
0008	4	FORMAT(F10.5,5X,13,F8.3)			
0009		K = 0			PHB014
0010		M = 0			PHB015
0011		SUMSHI = 0.			PHB016
0012		DO 10 I = 1,NSHIFT			PHB017
0013		READ(5,5) SHIFT,NMEASU			PHB018
0014	5	FORMAT(F10.5,5X,13)			PHB019
0015		SUMSHI = SUMSHI + SHIFT			PHB020
0016		DIMENSION COMNTS(9,50,7),IMPORT(20,50),TIMEXM(9,50),STRAIN(9,50),			PHB021
		MTRANS(9),CRISIS(20,20,7)			PHB022
0017		DO 20 J = 1, NMEASU			PHB023
0018		READ (5,6) TIME(I,J),GRAD(I,J),DIAL(I,J), IMPORT(I,J),(CRISIS(I,J),			PHB024
		IJJ),IJ = 1,7)			PHB025
0019	6	FORMAT(F9.2,1X,F5.1,3X,F8.5,2X,I2,7A4)			
0020		K = K + 1			PHB027
0021		IN(K) = K			PHB028
0022		IF (DIAL(I,J) .GT.0.) GO TO 12			PHB029
0023		DELTA = SCAFAC * GRAD(I,J) + SUMSHI			PHB030
0024		GO TO 11			PHB031
0025	12	DELTA = DIAL(I,J)			PHB032
0026		GO TO 11			PHB033
0027	11	TSTRAI = ALOG (1. + DELTA / ELNOT)			
	0	SELECTION OF COMMENTS			PHB035
0028		IF(IMPORT(I,J).GT.0) GO TO 13			PHB036
0029		GO TO 14			PHB037
0030	13	M = M + 1			PHB038
0031		DO 120 IJ = 1,7			PHB039
0032	120	COMNTS(L,M,IJ) = CRISIS(I,J,IJ)			PHB040
0033		IMPORT(L,M) = IMPORT(I,J)			PHB041
0034		TIMEXM(L,M) = TIME(I,J)			PHB042
0035		STRAIM(L,M) = TSTRAI			PHB043
0036		MTRANS(L) = M			PHB044
0037	14	STRAIN(K) = TSTRAI			PHB045
0038		TIMEX (K) = TIME(I,J)			PHB046
0039	20	CONTINUE			PHB047
0040	10	CONTINUE			PHB048
0041		H = K - 1			PHB049
0042		DO 30 I = 2, K			PHB050
0043		IF(I.F0.K) GO TO 32			PHB051
0044		RATE(I) = (STRAIN(I+1) - STRAIN(I-1)) / (TIMEX(I+1) -TIMEX(I-1))			PHB052
0045		GO TO 30			PHB053
0046	32	RATE(I)=(STRAIN(I)-STRAIN(I-1))/(TIMEX(I)-TIMEX(I-1))			PHB054
0047	30	CONTINUE			PHB055
0048		RATE(1) = RATE(2)			PHB056
	0	TRYING TO GET A DECENT OUTPUT			PHB057
0049		NUMERO = 0			PHB058

FORTRAN IV G COMPILER		MAIN	03-07-69	11:49:18	PAGE 0002
0050		1	1		PHB059
0051		1	1		PHB060
0052		1	1		PHB061
0053		1	1		PHB062
0054		1	1		PHB063
0055		1	1		PHB064
0056	41	1	1		PHB065
0057	42	1	1		PHB066
0058		1	1		PHB067
0059		1	1		PHB068
0060	2	1	1		PHB069
		1	1		PHB070
		1	1		PHB071
0061		1	1		PHB072
0062		1	1		PHB073
0063	43	1	1		PHB074
0064	46	1	1		PHB075
0065		1	1		PHB076
0066		1	1		PHB077
0067		1	1		PHB078
0068	44	1	1		PHB079
0069	7	1	1		PHB080
0070	45	1	1		PHB081
0071	3	1	1		PHB082
0072	130	1	1		PHB083
0073		1	1		PHB084
0074		1	1		PHB085
0075		1	1		PHB086
0076	9	1	1		PHB087
0077	40	1	1		PHB088
	C	1	1		PHB089
0078		1	1		PHB090
0079		1	1		PHB091
0080		1	1		PHB092
0081		1	1		PHB093
0082		1	1		PHB094
0083	70	1	1		PHB095
0084		1	1		PHB096
0085		1	1		PHB097
0086	100	1	1		PHB098
0087		1	1		PHB099
0088	60	1	1		PHB100
0089		1	1		PHB101
	C	1	1		PHB102
	C	1	1		PHB103
	C	1	1		PHB104
0090		1	1		PHB105
0091		1	1		PHB106
0092		1	1		PHB107
0093		1	1		PHB108
0094		1	1		PHB109
0095		1	1		PHB110
0096		1	1		PHB112
0097	90	1	1		PHB113
0098		1	1		PHB114

FORTRAN IV C COMPILER		MAIN	03-17-69	18:31:04	PAGE 0003
0099		TITLE (1) = TIT(L,1)			PHB115
0100	110	CONTINUE			PHB116
0101		CALL TIME (XC,YC,5,1)			PHB117
0102		WRITE(6,1000) XC,YC			
0103	1000	FORMAT(12F6.2)			
0104		CALL PLGT (1,0,-3)			PHB118
0105		CALL SCALE (TIME,K,10.,XMIN,DX,1)			PHB119
0106		CALL SCALE (STRAIN,K,7.,YMIN,DY,1)			PHB120
0107		CALL SCALE (RATE,K,7.,ZMIN,DZ,1)			PHB121
0108		DO 50 I = 1,K			PHB122
0109		RATE (I) = RATE(I) + 1.			PHB123
0110		STRAIN(I) = STRAIN(I) + 1.			PHB124
0111		WRITE(6,1000) TIME(X(I),STRAIN(I),RATE(I)			
0112	50	CONTINUE			PHB125
0113		CALL AXIS (0.,1.,18H TIME HOUR,-18,10.,0.,XMIN,DX)			PHB126
0114		CALL AXIS (0.,1.,12H STRAIN ,12,7.,90.,YMIN,DY)			PHB127
0115		CALL LINE (TIME,STRAIN,K,1)			PHB128
0116		XO = TIME(K) - .4			PHB129
0117		YO = STRAIN(K) + .1			PHB130
0118		CALL SYMBOL (XO,YO,.07,6HSTRAIN,0.,6)			PHB131
0119		CALL AXIS (10.,1.,25H STRAIN RATE 1/HOUR,-25,7.,90.,ZMIN,DZ)			PHB132
0120		CALL LINE (TIME,RATE,K,1)			PHB133
0121		ZO = RATE(K) + .5			PHB134
0122		CALL SYMBOL (XO,ZO, .07,11HSTRAIN RATE,0.,11)			PHB135
0123		CALL SYMBOL (1.,8.,.14,TITLE,0.,80)			PHB136
	C				PHB137
	C	PRINTING OF COMMENTS			PHB138
	C				PHB139
0124		M = MTRANS(L)			PHB140
0125		DIMENSION TIMM(50),STRAM(50),XF(6),YF(6), XE(2),YE(2),COM1(4),COMPHB141			
		12(3),LEAP(50)			PHB142
0126		DO 9999 I=1,6			
0127		XF(I)=0.			
0128	9999	YF(I)=0.			
0129		XE(1)=0.			
0130		XE(2)=0.			
0131		YE(1)=0.			
0132		YE(2)=0.			
0133		SPACIN = 0.			PHB143
0134		ALTITU = 0.			PHB144
0135		DISTAN = 1.			PHB150
0136		KOUNT=0			
0137		WRITE(6,1002) KOUNT			
0138	1002	FORMAT(I6)			
0139		DO 140 J = 1,M			PHB151
0140		TIMM(J) = (TIME(X(L,J) - XMIN) / DX			PHB152
0141		STRAM(J) = (STRAIN(L,J) - YMIN) / DY + 1.			PHB153
0142		XF(1) = TIMM(J)			PHB154
0143		XF(2) = XF(1) + .02			PHB155
0144		XF(3) = XF(1)			PHB156
0145		XF(4) = XF(1) - .02			PHB157
0146		XF(5) = XF(1)			PHB158
0147		XF(6) = XF(1)			PHB159
0148		LOGICAL MIDDLE, PLACE,CLEAR			PHB160
0149		MIDDLE = STRAM(J) .GT.5.			PHB161

FORTRAN IV G COMPILER		MAIN	03-17-69	18:31:04	PAGE 0004
0150		PLACE = IMPOST(L,J) .LT.2			PHB162
0151		IF (J.GT.1) GO TO 143			PHB163
0152		GO TO 144			PHB164
0153	143	DISTAN = TIMM(J) - TIMOUT			PHB165
0154		IF (DISTAN .LT..2) GO TO 145			PHB166
0155	144	XE(1) = TIMM(J)			PHB167
0156		IF (XE(1) .LT. .1) TIMM(J) = .1			PHB168
0157		IF (XE(1) .GT. 9.85) TIMM(J) = 9.85			PHB169
0158		XE(2) = TIMM(J)			PHB170
0159		XD1 = XE(2)			PHB171
0160		XD2 = XE(2) + .1			PHB172
0161	141	IF (MIDDLE) GO TO 146			PHB173
0162		YE(1) = 5.8			PHB174
0163		YE(2) = 6.			PHB175
0164		YD1 = YE(2)			PHB176
0165		YE(1) = STRAM(J) + .08			PHB177
0166		YE(6) = STRAM(J) + .25			PHB178
0167		KOUNT=KOUNT+1			
0168		WRITE(6,1002) KOUNT			
0169		GO TO 147			PHB179
0170	146	YE(1) = 3.7			PHB180
0171		YE(2) = 3.5			PHB181
0172		YD1 = 2.06			PHB182
0173		YE(1) = STRAM(J) - .08			PHB183
0174		YE(6) = STRAM(J) - .25			PHB184
0175	147	YD2 = YD1			PHB185
0176		ANGLE = 90.			PHB186
0177		LEAP(J) = 0			PHB187
0178		KOUNT=KOUNT+1			
0179		WRITE(6,1002) KOUNT			
0180		IF(DISTAN .LT. .2 .AND. PLACE) GO TO 142			PHB188
0181		GO TO 148			PHB189
0182	145	IF (PLACE) GO TO 141			PHB190
0183		IF (TIMM(J) .GT. .72) GO TO 151			PHB191
0184		XD1 = .1			PHB192
0185		GO TO 152			PHB194
0186	151	IF (TIMM(J) .GT. 9.27) GO TO 153			PHB195
0187		XD1 = TIMM(J) - .72			PHB196
0188		GO TO 152			PHB198
0189	153	XD1 = 8.55			PHB199
0190	152	XD2 = XD1			PHB201
0191		XE(1) = TIMM(J)			PHB202
0192		XE(2) = TIMM(J)			PHB203
0193		ROOM = TIMM(J) - SPACIN			PHB204
0194		CLEAR = ROOM .GT. 1.44 .OR. VCLEAR .GT. .2			PHB205
0195		VCLEAR = STRAM(J) - ALTITU			PHB206
0196		SPACIN = TIMM(J)			PHB207
0197		ALTITU = STRAM(J)			PHB208
0198		KOUNT=KOUNT+1			
0199		WRITE(6,1002) KOUNT			
0200		IF (MIDDLE) GO TO 154			PHB209
0201		IF (.NOT. CLEAR) GO TO 157			PHB210
0202	156	IF (LEAP(J-1) .EQ. 1) GO TO 158			PHB211
0203	159	YE(1) = STRAM(J) + .08			PHB212
0204		LEAP(J) = 1			PHB213

FORTRAN IV C COMPILER		MAIN	03-17-69	18:31:04	PAGE 0005
0205		YF(6) = STRAM(J) + .25			PHB214
0206		YF(1) = YF(6) + .2			PHB215
0207		YF(2) = YF(6) + .4			PHB216
0208		YD1 = YF(2) + .1			PHB217
0209		YD2 = YF(2)			PHB218
0210		KOUNT=KOUNT+1			
0211		WRITE(6,1002) KOUNT			
0212		GO TO 155			PHB220
0213	154	IF (.NOT. CLEAR) GO TO 156			PHB221
0214	157	IF (LEAP(J-1) .EQ. 2) GO TO 159			PHB222
0215	158	YF(1) = STRAM(J) - .08			PHB223
0216		LEAP(J) = 2			PHB224
0217		YF(6) = STRAM(J) - .25			PHB225
0218		YF(1) = YF(6) - .2			PHB226
0219		YF(2) = YF(6) - .4			PHB227
0220		YD1 = YF(2) - .1			PHB228
0221	155	ANGLE = 0.			PHB230
0222		YD2 = YF(2) - .2			PHB231
0223		KOUNT=KOUNT+1			
0224		WRITE(6,1002) KOUNT			
0225	148	DO 160 I = 1,4			PHB232
0226	160	COM1(I) = COMNTS(L,J,I)			PHB233
0227		DO 170 I = 5,7			PHB234
0228		IA = I - 4			PHB235
0229	170	COM2(IA) = COMNTS(L,J,I)			PHB236
0230		CALL LINE (XE,YE,2,1)			PHB237
0231		WRITE(6,1000) XE,YE			
0232		CALL SYMBOL (XD1 ,YD1 , .07,COM1,ANGLE,24)			PHB238
0233		CALL SYMBOL (XD2,YD2,.07,COM2,ANGLE,18)			PHB239
0234		WRITE(6,1000) XD1,XD2,YD1,YD2			
0235		TIMOUT = TIMM(J)			PHB240
0236	142	YF(2) = YF(1)			PHB241
0237		YF(3) = STRAM(J)			PHB242
0238		YF(4) = YF(1)			PHB243
0239		YF(5) = YF(1)			PHB244
0240		CALL LINE (XF, YF, 6,1)			PHB245
0241		WRITE(6,1000) XF,YF			
0242	140	CONTINUE			PHB251
	C	THE END OF COMMENTS			PHB252
0243		CALL PLOT (12,.0,-3)			PHB253
0244	80	CONTINUE			PHB256
0245		CALL PLOTND			PHB257
0246		STOP			PHB258
0247		END			PHB259

APPENDIX II

Additional Creep Curves

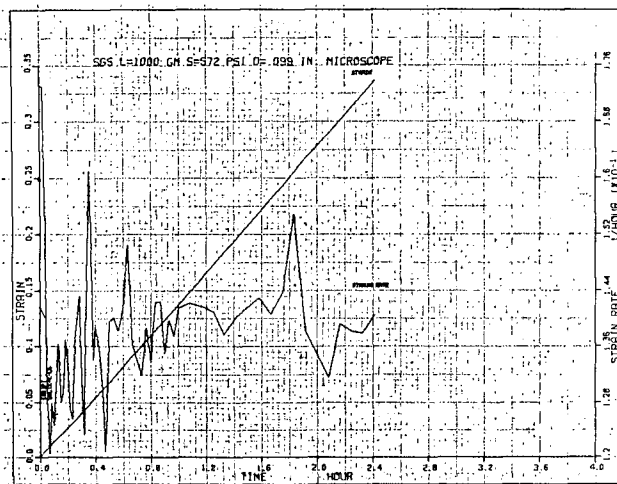


Figure a. Stage II (SGS), 572 psi.

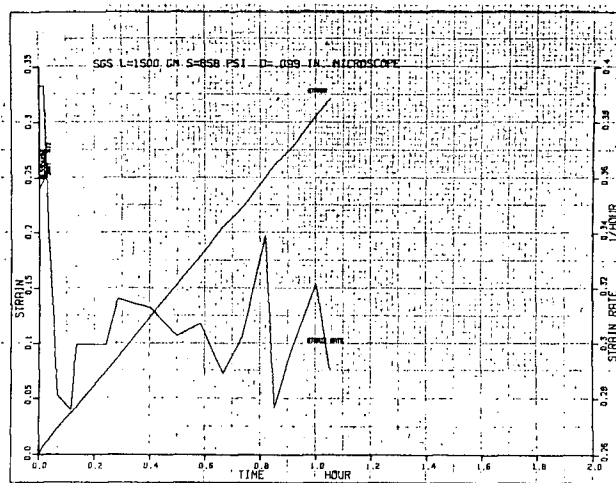


Figure b. Stage II (SGS), 858 psi.

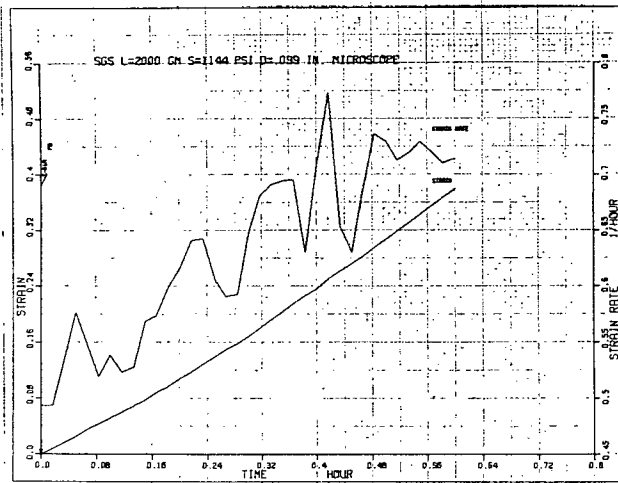


Figure c. Stage II (SGS), 1144 psi

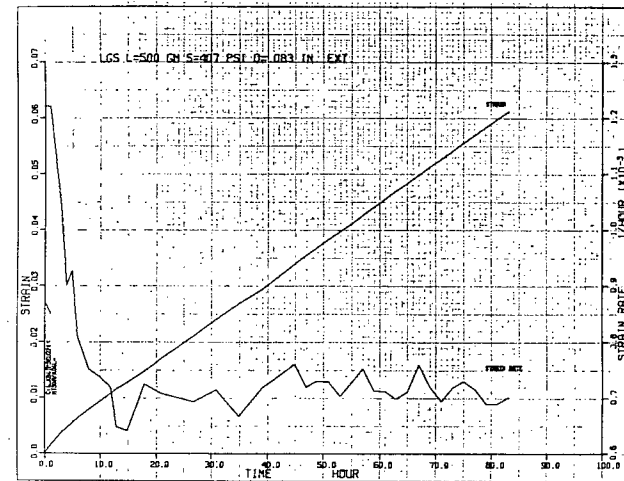


Figure d. Stage II (LGS), 407 psi.

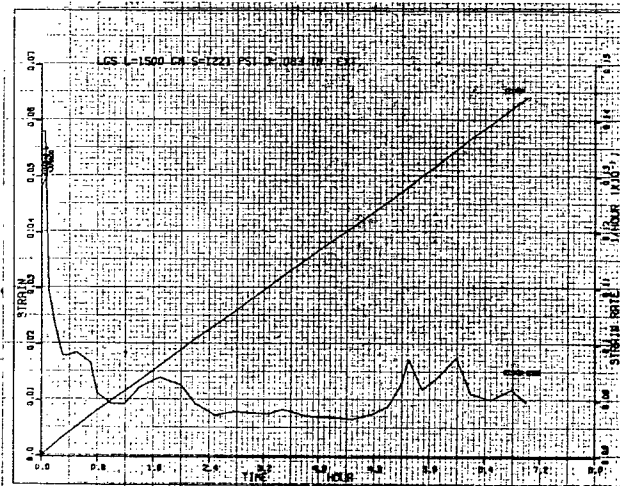


Figure e. Stage II (LGS), 1221 psi

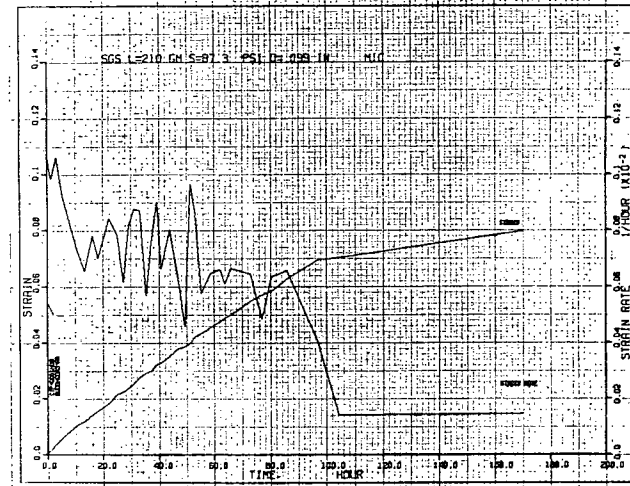


Figure f. Stage I (SGS), 120 psi.

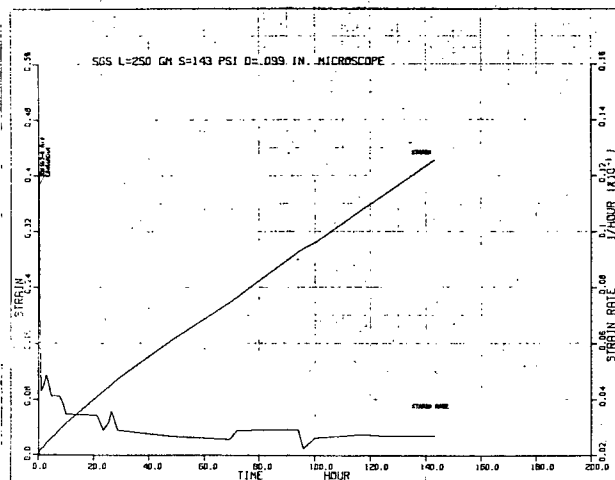


Figure g. Stage I (SGS), 143 psi

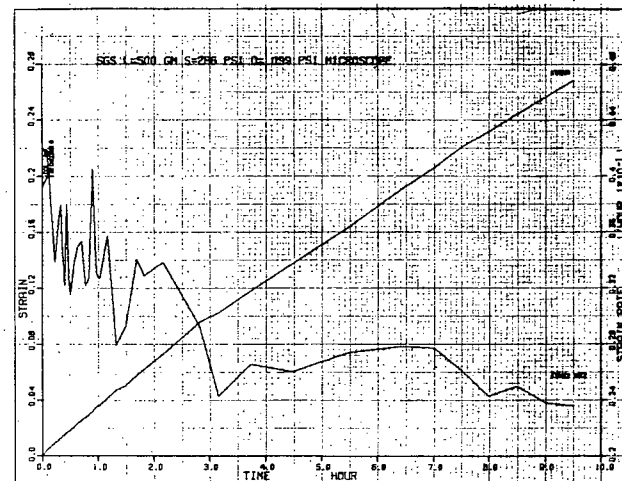


Figure h. Stage I (SGS), 286 psi.

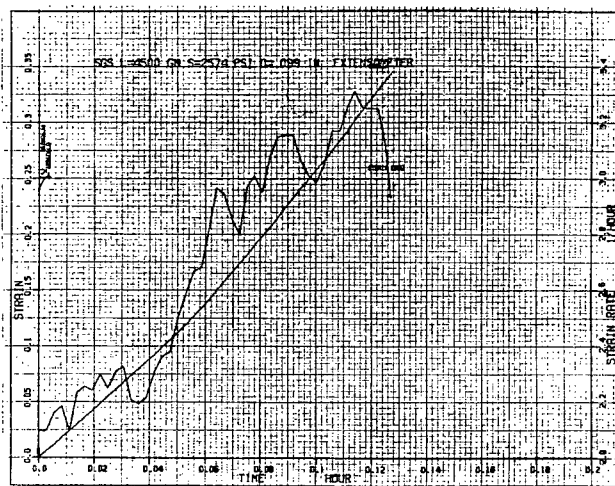


Figure i. Transition (SGS), 2574 psi.

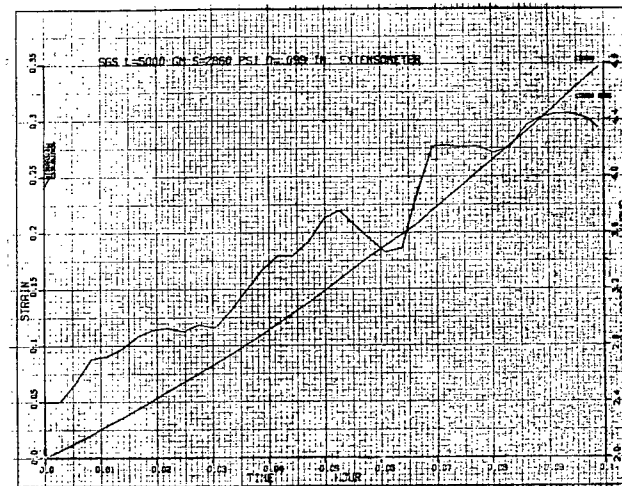


Figure j. Transition (SGS), 2860 psi.

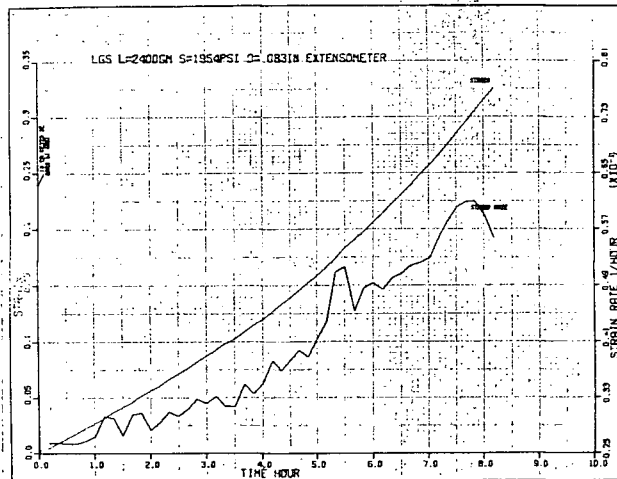


Figure k. Transition (LGS). 1954 psi.

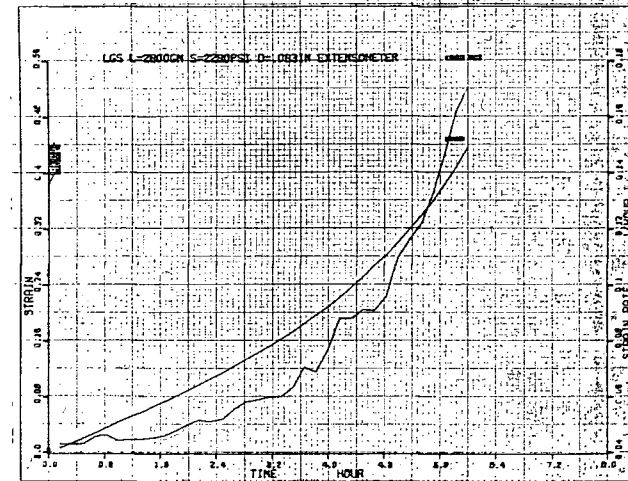


Figure l. Transition (LGS), 2280 psi.

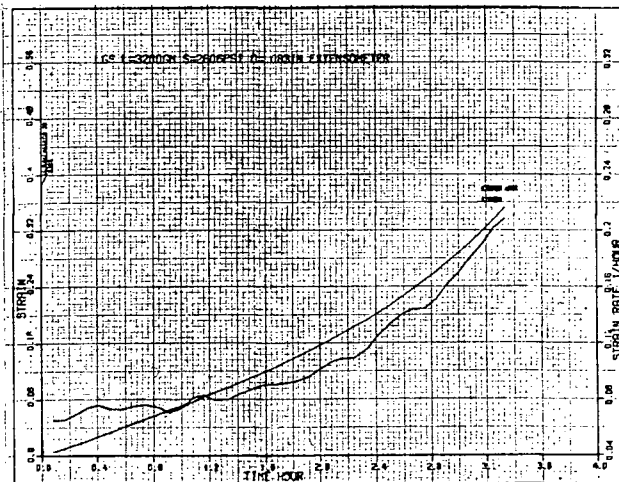


Figure m. Transition (LGS), 2606 psi.

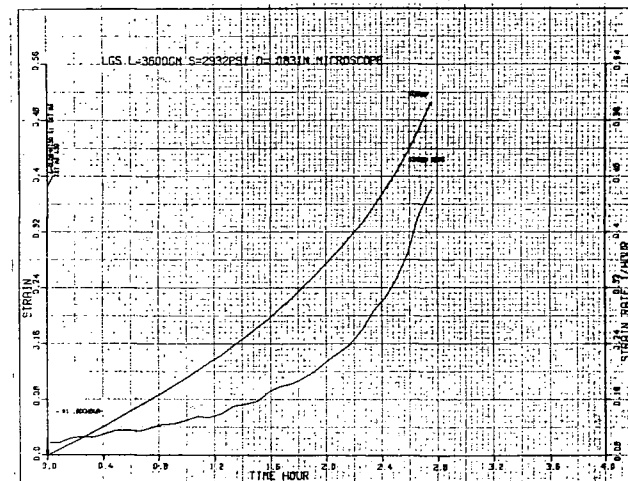


Figure n. Transition (LGS), 2932 psi.

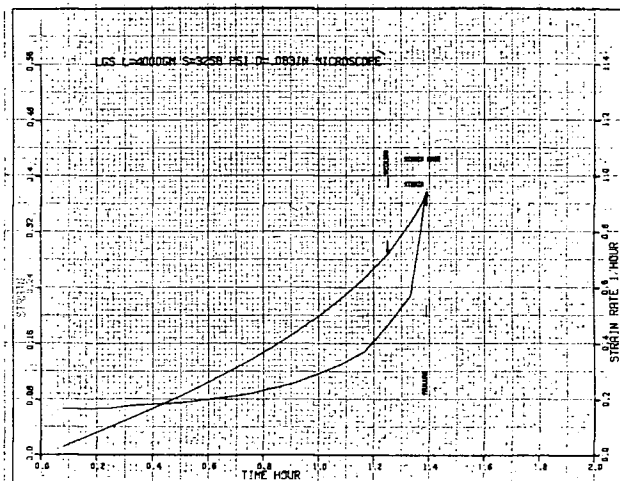


Figure o. Transition (LGS), 3258 psi.

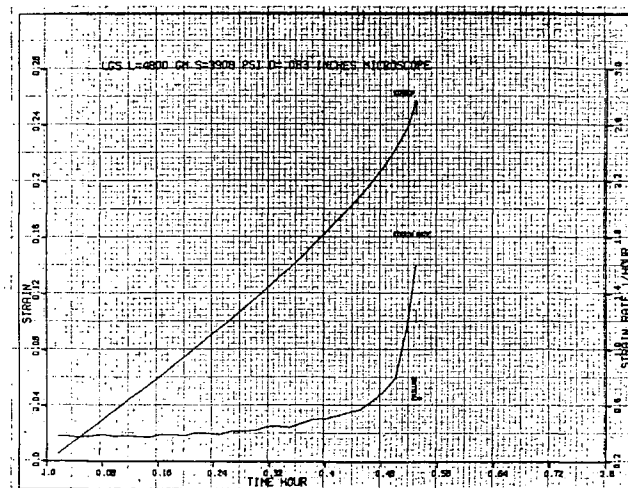


Figure p. Transition (LGS), 3908 psi.

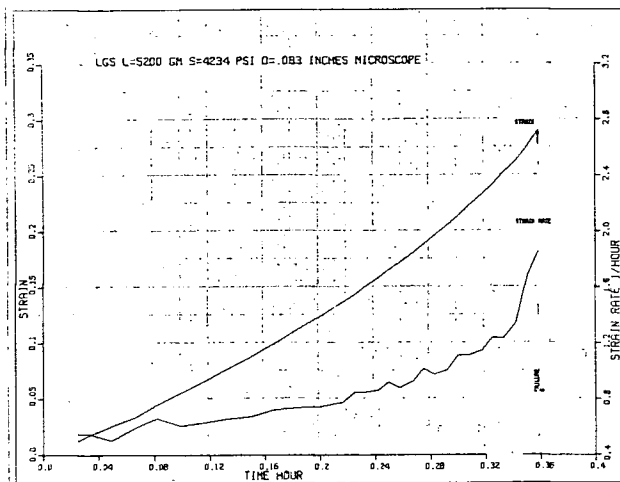


Figure q. Transition (LGS), 4234 psi.

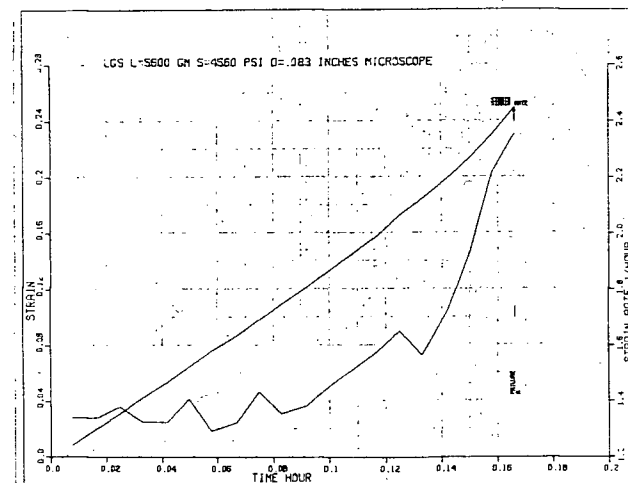


Figure r. Transition (LGS), 4560 psi.

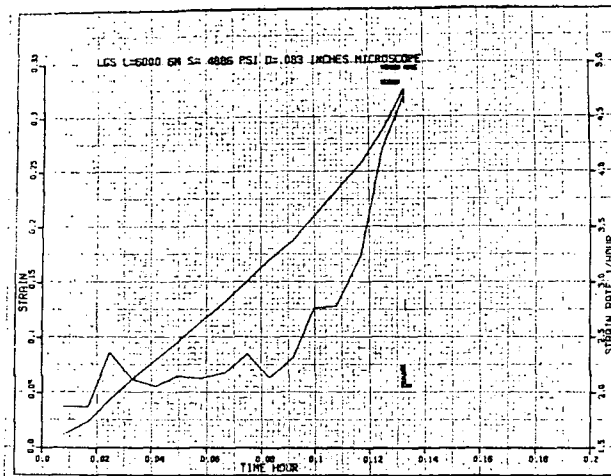


Figure s. Transition (LGS), 4886 psi.

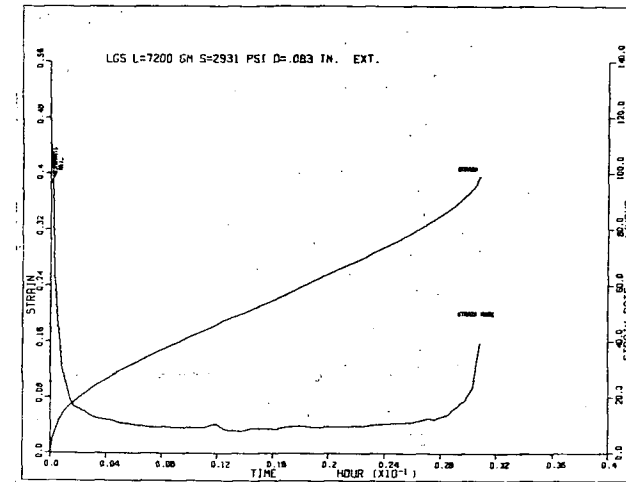


Figure t. Stage III, 2931 psi.

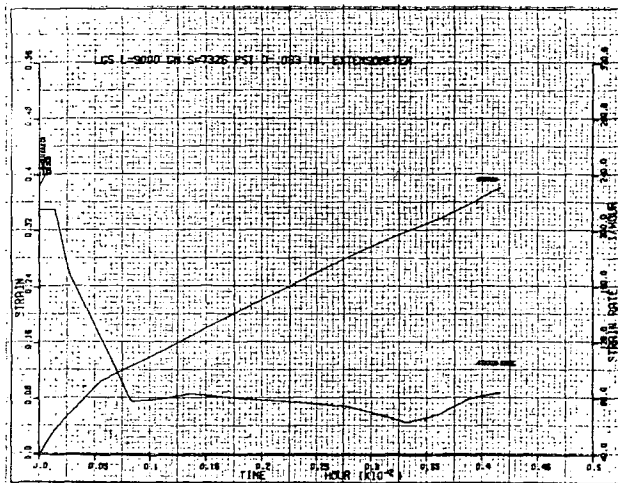


Figure u. Stage III, 7326 psi.

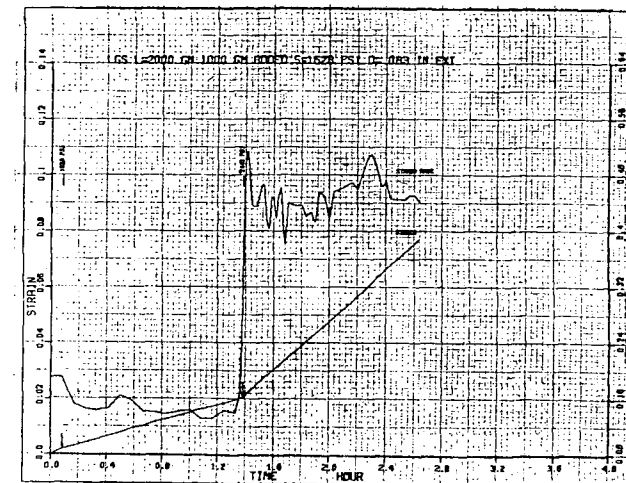


Figure v. Stage II incremental loading.

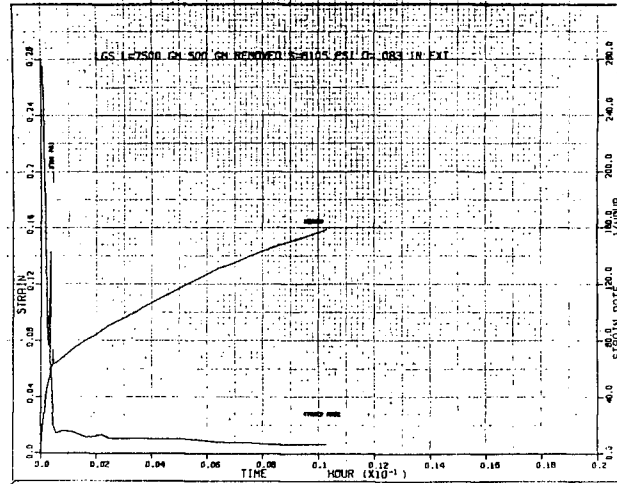


Figure w. Stage III unloading.

APPENDIX III

Calculation of Theoretical Creep Curves for Pure Nabarro-Herring Creep and Pure Coble Creep.

N-H.

Assume that a grain deforms only by N-H diffusional creep.

Initial length = l_0

Initial widths = w_0

Increases in length = Δl

Increase in width = Δw

Final length l = $l_0 + \Delta l$

Final width w = $w_0 + \Delta w$

Engineering strain = $\frac{\Delta l}{l_0} = E$

True strain $d\epsilon$ = dl/l ; $\epsilon = \ln \frac{l}{l_0} = \ln \left(1 + \frac{\Delta l}{l_0} \right) = \ln (1 + E)$

$$E + 1 = e^\epsilon \quad \text{or} \quad E = e^\epsilon - 1$$

For constant volume

$$\epsilon_1 + \epsilon_2 + \epsilon_3 = 0$$

Assume $\epsilon_2 = \epsilon_3 = -\frac{1}{2}\epsilon_1$ with a Poissons ratio of $\frac{1}{2}$ for plastic deformation.

$$\ln \left(1 + \frac{\Delta w}{w_0} \right) = -\frac{1}{2} \ln \left(1 + \frac{\Delta l}{l_0} \right)$$

$$\ln \left(1 + \frac{\Delta w}{w_0} \right) = \ln \left(1 + \frac{\Delta l}{l_0} \right)^{-1/2}$$

$$(1 + E_T) = (1 + E_L)^{-1/2}$$

Assume initial grain dimensions l_0, w_0

After engineering strain E_L

$$L = L_0(1 + E_L) = L_0 e^E$$

$$W = W_0(1 + E_2)^{-1/2} = W_0 e^{-E/2}$$

Define grain size \bar{L} where $\bar{L}^2 = \frac{1}{2}(L^2 r w^2) = \frac{1}{2}L_0^2 e^{2E} + \frac{1}{2}W_0^2 e^{-E}$

If the grain is initially equiaxed

$$\bar{L}^2 = \frac{1}{2}L_0^2 \{e^{2E} + e^{-E}\}$$

From Zehr and Backofen¹⁰

$$\frac{\sigma}{E} = \mathcal{N} N \cdot H \approx \frac{L^2 kT}{\alpha v D_L}$$

where α is a geometrical constant ≈ 10

v is the atomic volume ($1.43 \times 10^{-23} \text{ cm}^3$ for Sn)

D_L is the coefficient for lattice diffusion

k is Boltzman's constant $= 1.38 \times 10^{-16} \text{ erg/}^\circ\text{K}$

T is the absolute temperature ($^\circ\text{K}$)

Pure N-H creep is much slower than that found experimentally. Values of D_L for Sn will give the fastest rate. If the grain size is 2 microns and $T = 26^\circ\text{C}$.

$$\mathcal{N} N \cdot H = 2.74 \times 10^{17} \frac{\text{dynes} \cdot \text{-sec}}{\text{cm}^2} = 3.96 \times 10^{12} \text{ lb-sec/in}^2$$

$$dE = \frac{\sigma}{\mathcal{N} N \cdot H} dt$$

$$\int_0^E \bar{L}^2 dE = \int_0^t \frac{v \sigma \alpha D_L}{kT} dt$$

$$\sigma \left(\frac{\alpha v D_L}{kT} \right) t = \frac{1}{2} L_0^2 \int_0^E (e^{2E} + e^{-E}) dE = \frac{1}{2} L_0^2 \left\{ \frac{e^{2E}}{2} + e^{-E} + \frac{1}{2} \right\}$$

$$t = \frac{\mathcal{N} N \cdot H}{4s} \{e^{2E} - 2e^{-E} + 1\}$$

$$\sigma = 97 \text{ psi}$$

$$\mathcal{N}_{N-H} = 3.96 \times 10^{12} \frac{\text{lb-sec}}{\text{in}^2} \times \frac{\text{hr}}{3600 \text{ sec}} = 1.1 \times 10^9 \frac{\text{lb-hr}}{\text{in}^2}$$

$$t = \frac{1.1 \times 10^9}{4 \times 97} \{e^{2\epsilon} - 2e^{-\epsilon} + 1\}$$

$$t = 2.85 \times 10^5 \{e^{2\epsilon} - 2e^{-\epsilon} + 1\} \text{ hrs.}$$

N-H Creep

<u>True Strain</u>	<u>Time (hrs)</u>	<u>Fraction of time to reach .40 strain</u>
0	0	0
.01	1.14×10^4	2.1
.02	2.28×10^4	4.2
.05	5.70×10^4	10.6
.10	1.16×10^5	21.5
.20	2.42×10^5	45.0
.30	3.82×10^5	71.0
.40	5.39×10^5	100.0

Coble

The analysis is similar to that for N-H creep.

Grain size is identified as

$$\bar{L}^3 = \frac{1}{2} (L_o^3 + W_o^3) = \frac{1}{2} L_o^3 e^{3\epsilon} + \frac{1}{2} W_o^3 e^{-3/2\epsilon}$$

for equiaxed grains $L_o = W_o$

$$\bar{L}^3 = \frac{1}{2} L_o^3 (e^{3\epsilon} + e^{-3/2\epsilon})$$

$$\frac{\sigma}{\epsilon} = \mathcal{N}_{co} \approx \frac{L^3 kT}{\beta v_w D_{gb}}$$

where D_{gb} is the grain boundary diffusion coefficient

β is a constant ≈ 150

w is grain boundary width ($\sim 10^{-7}$ cm)

T is 26° C

L is 2 microns

σ is 97 psi

$\mathcal{N}_{co} = \mathcal{N}_{pb} = 3.88 \times 10^{10}$ dynes sec/cm² since coble creep is much faster than the experimental rate and \mathcal{N}_{pb} gives a slower rate of creep than \mathcal{N}_{Sn} .

$$\int_0^\epsilon \bar{L}^3 d\epsilon = \int_0^t \frac{\sigma \beta v w D_{gb}}{kT} dt$$

$$\frac{L_0^3}{2} \int_0^\epsilon (e^{3\epsilon} + e^{-3/2\epsilon}) d\epsilon = \left(\frac{\sigma \beta v w D_{gb}}{kT} \right) t$$

$$t = \frac{L_0^3 kT}{\beta v w D_{gb}} \left(\frac{1}{6\sigma} \right) \left[e^{3\epsilon} - 2e^{-3/2\epsilon} + 1 \right]$$

$$t = \frac{L_0^3 kT}{\beta v w D_{gb}} \left(\frac{1}{6\sigma} \right) \left[e^{3\epsilon} - 2e^{-3/2\epsilon} + 1 \right]$$

$$t = .27 \left[e^{3\epsilon} - 2e^{-3/2\epsilon} + 1 \right] \text{ hrs.}$$

Coble Creep

<u>True Strain</u>	<u>Time (hrs)</u>	<u>Fraction of time to reach .40 strain</u>
0	0	0
.01	1.62×10^{-2}	.0187
.02	3.24×10^{-2}	.0374
.05	8.4×10^{-2}	.096
.10	1.7×10^{-1}	.196
.20	3.6×10^{-1}	.415
.30	5.9×10^{-1}	.680
.40	8.7×10^{-1}	1.00

BIBLIOGRAPHY

1. D. Lee, G.E. Res. and Dev. Center Report #69-C-005.
2. C.E. Pearson, J. Inst. Metals, 54 (1934).
3. D.H. Avery and W.A. Backofen, ASM Tran. Quart., 58 (1965) 551.
4. D. Lee and W.A. Backofen, Trans. AIME, 239 (1967) 1034.
5. T.H. Alden, Acta. Met., 15 (1967) 469.
6. H.E. Cline and T.H. Alden, Trans. AIME., 239 (1967) 710.
7. D.L. Holt and W.A. Backofen, ASM Trans. Quart., 59 (1966) 755.
8. T.H. Alden and H.W. Schadler, Trans. AIME., 242 (1968) 825.
9. P.J. Martin and W.A. Backofen, ASM Trans. Quart., 60(1967) 352.
10. S.W. Zehr and W.A. Backofen, ASM Trans. Quart. , 6(1968) 300.
11. D.L. Holt, Trans. AIME, 242 (1968) 25.
12. H.W. Hayden, R.C. Gibson, H.F. Merrick and J.H. Brophy, ASM Trans. Quart., 60, 3 (1967).
13. T.H. Alden, ASM Trans. Quart., 61 (1968) 559.
14. T.H. Alden, Trans. AIME, 236 (1966) 1633..
15. R.C. Grifkins, J. Inst. Metals, 95 (1967) 373.
16. R.C. Cook, M.A.Sc. Thesis, University of British Columbia.
17. S. Floreen, Scripta Met., 1 (1967) 19.
18. W.A. Backofen, I.R. Turner, and D.H. Avery, ASM Trans. Quart., 57 (1964) 980.
19. Private communication with T.H. Alden.
20. A.K. Head, Phil. Mag., 44, (1953) 92.
21. A.K. Head, Proc. Phys. Soc. (London), 1366 (1953) 793.
22. Y. Ishida and M.H. Brown, Acta Met., 15 (1967) 857.
13. H. Gleiter, E. Hornbogen and G. Baro, Acta Met. , 16 (1968) 1053.

24. R.G. Gifkins and K.V. Snowden, Trans. AIME, 239 (1967) 105.
25. S.K. Tung and R. Maddin, Trans. AIME, 109 (1967) 905.
26. P.R. Strutt, A.M. Lewis and R.C. Gifkins, J. Inst. Metals, 93 (1964) 71.
27. R.B. Jones and R.H. Johnson, Discussion, ASM. Trans. Quart., 59 (1966) 356.
28. W.A. Backofen et al in Ductility, ASM, Metals Park, (1968) 279.
29. A. Karim, D.L. Holt and W.A. Backofen, Trans AIME, 245 (1969) 1131.
30. P. Chaudhari, IBM Research Report, RC 1946.
31. T.H. Alden, "Interaction of Dislocations and Grain Boundaries During Superplastic creep", International Conference, "Interfaces", Melbourne, Australia, August, 1969.
32. P. Chaudhari, Acta Met., 15 (1967) 1777.
33. E.N. Andrade and K.H. Joliffe, Proc. Roy. Soc. (London) A 254 (1960) 291.
34. R.C. Gifkins, Trans AIME, 215 (1969) 1015.
35. S. Bhattacharya, W.K.A. Congreve and F.C. Thompson, J. Inst. Metals, 81 (1952) 83.
36. J.E. Breen and J. Weertman, J. Metals, 7 (1955) 1230.
37. F. Garofalo, Fundamentals of Creep and Creep-Rupture in Metals, N.Y. McMillan (1965).
38. C.M. Packer, R.H. Sohnsen and O.D. Sherby, Trans AIME., 242 (1968) 2485.
39. R. Kossowsky and S.H. Bechtold, Trans AIME, 242 (1968) 716.
40. D. McLean, Trans AIME, 242 (1968) 1193.
41. P. Chaudhari, Science and Technology, Sept. 1968, P.42.
42. H.J. McQueen, W.A. Wong, and J.J. Jones, Can. J. Phys., 45 (1967) 1225.
43. R.C. Gifkins, J. Inst. Metals, 79 (1951) 233.
44. W.A. Wood, G.R. Wilms and W.A. Rachinger, J. Inst. Metals, 79 (1951) 159.
45. T.H. Alden, "Dislocation Climb Theories of Creep and Superplasticity", (1969).
46. C.M. Parker and O.D. Sherby, ASM Trans. Quart., 60 (1967) 21.
47. Private communication with K.C. Donaldson.